Co-axial vs. Multi-axial beam combination

Co-axial: pairwise combinations using beam splitters

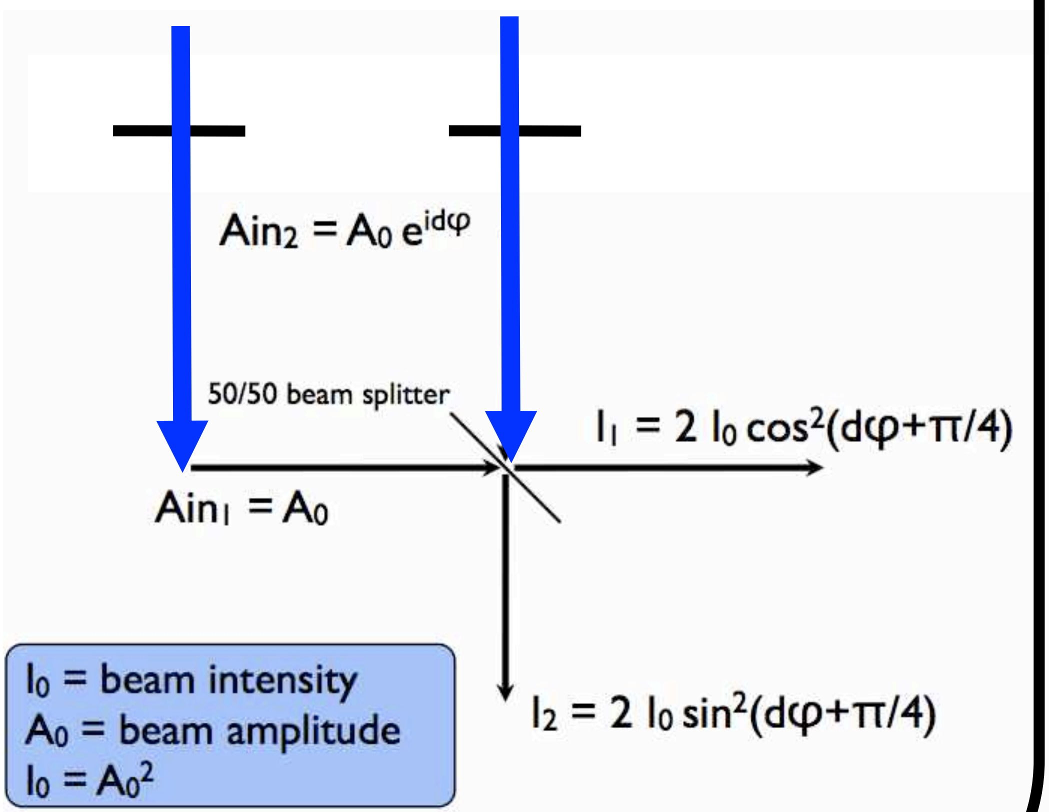

Multi-axial: beams sent to a single imaging optical system

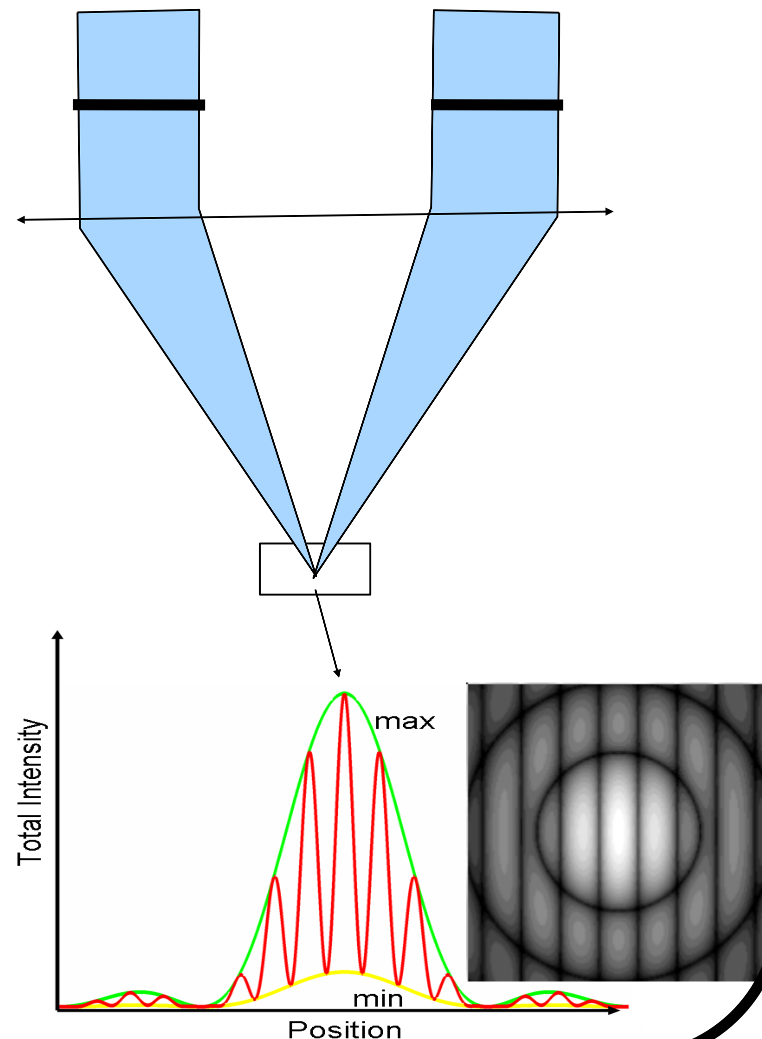

Co-axial vs. Multi-axial beam combination

Co-axial combination
Advantages:

- Efficient use of detector pixels
- Each beam is treated as a single mode
  - → spatial filtering techniques can be used (fibers, pinholes) to clean beams
  - → easy to transport beams over large distances
  - → high accuracy calibration is possible

Limitations:

- Information across individual apertures is erased
- small field of view (usually limited to diffraction limit of a single aperture)
- becomes complicated with large number of apertures: number of beam splitters grows as $\sim N^2$

Co-axial combination is usually preferred for long baselines / single object interferometry.
Most current interferometers use co-axial combination

Examples: CHARA, Keck, VLTI

Multi-axial (Fizeau) combination is required for wide field of view, and is attractive when telescopes aperture is comparable to baseline

Example : LBTI

Combining beams with beam splitters

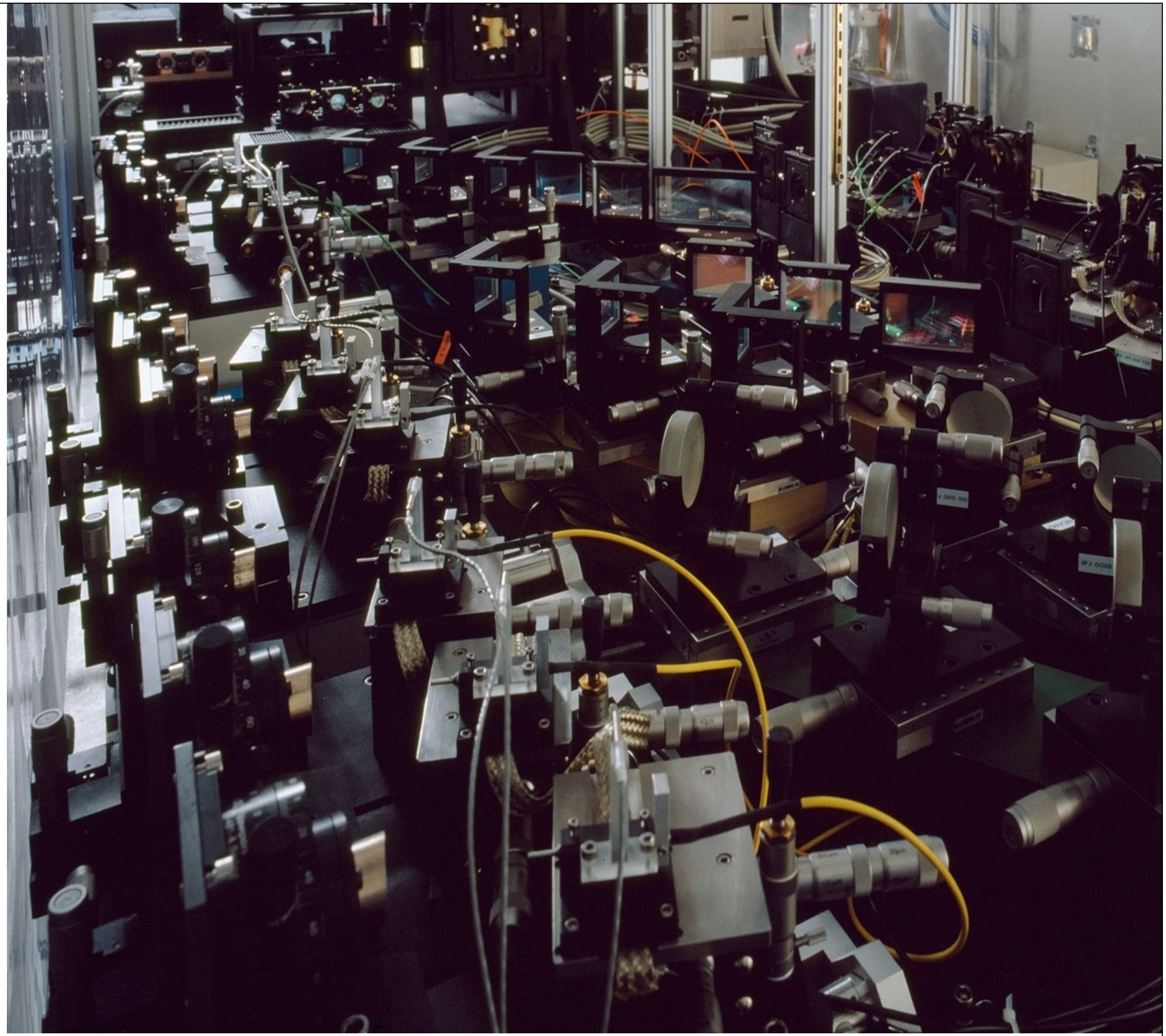

AMBER beam combining optics (VLT, ESO)
Several beam splitters are seen in this picture

LBTI on the LBT

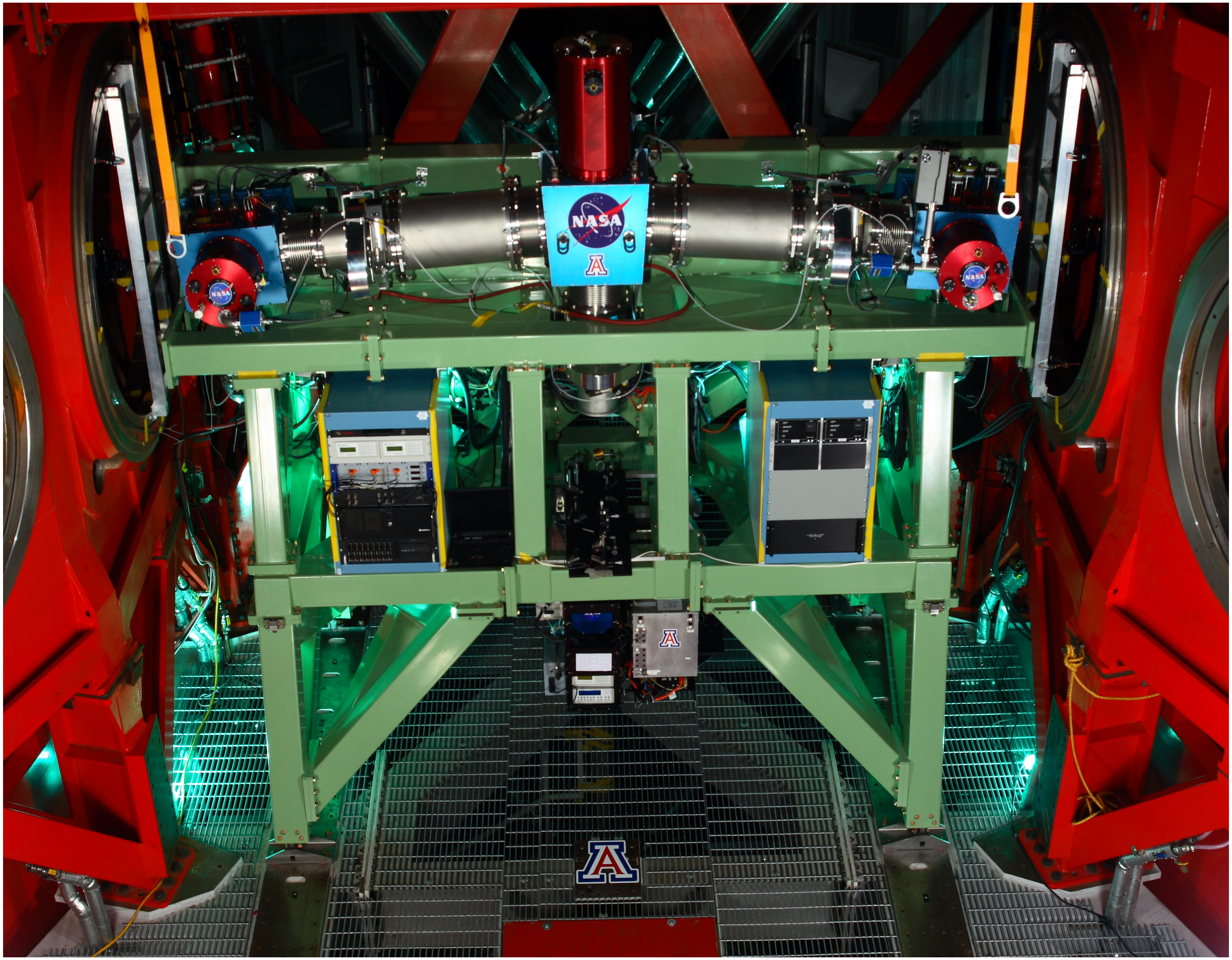

The Sine Condition (also called the golden rule)

Properly designed imaging systems obey the sine condition for the relation of the object plane to the image plane. For imaging systems with the object at infinity the relation becomes

$$\sin \alpha = h/f$$

where h is the height of the ray from the optical axis and f is the focal length of the system.

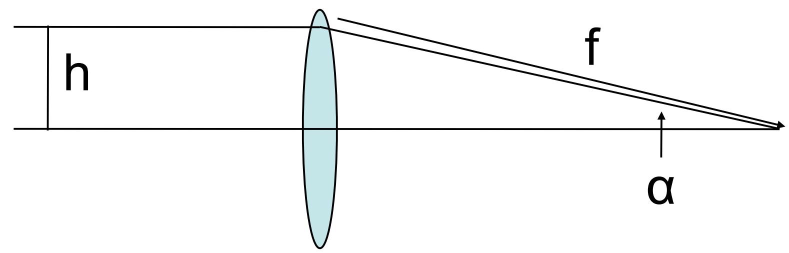

For interferometers, obeying this design constraint results in interference fringes for a source anywhere in the focal plane.

For interferometers not obeying this constraint the field is much smaller.

Example: Michelson's Stellar Interferometer

Combined beams

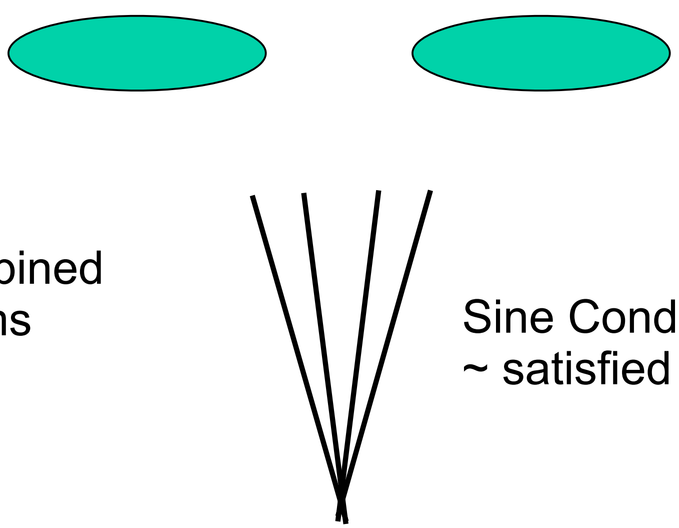

Sine Condition ~ satisfied

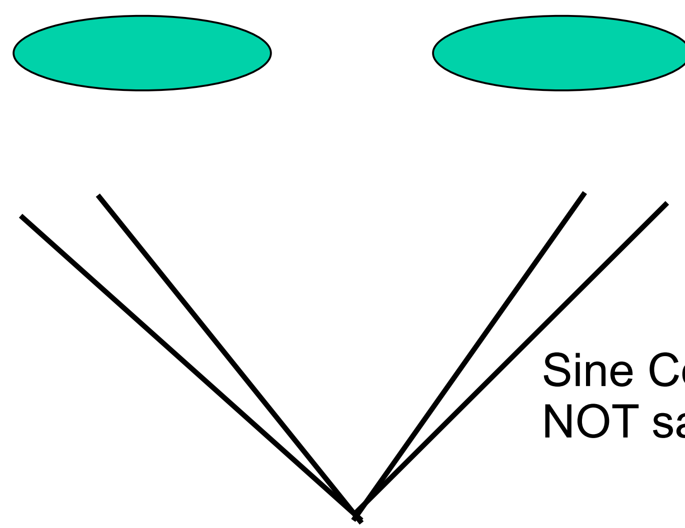

Sine Condition NOT satisfied

Multi-Axial Beam Combination (LBTI first fringes)

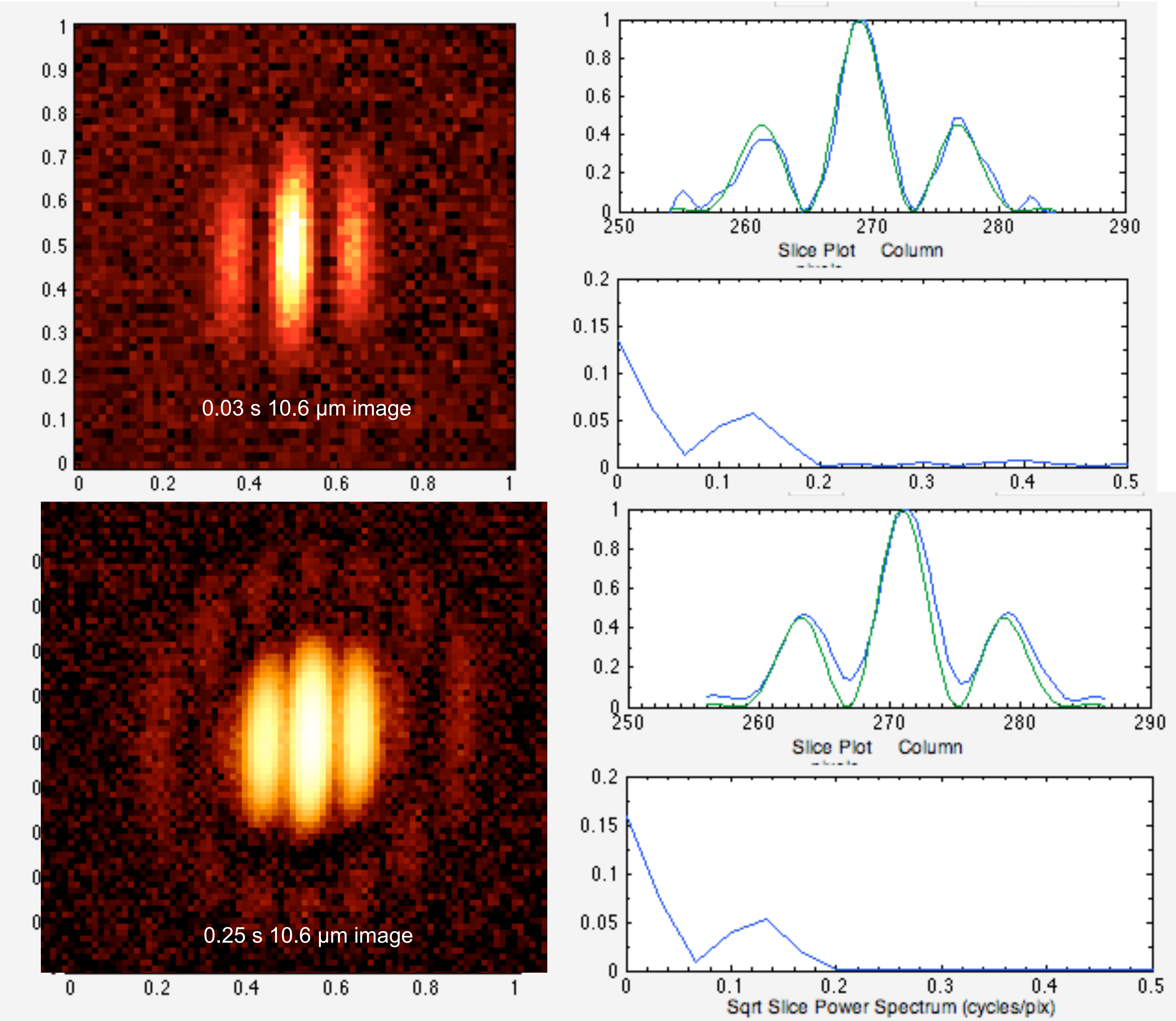

Atmospheric Phase Variations

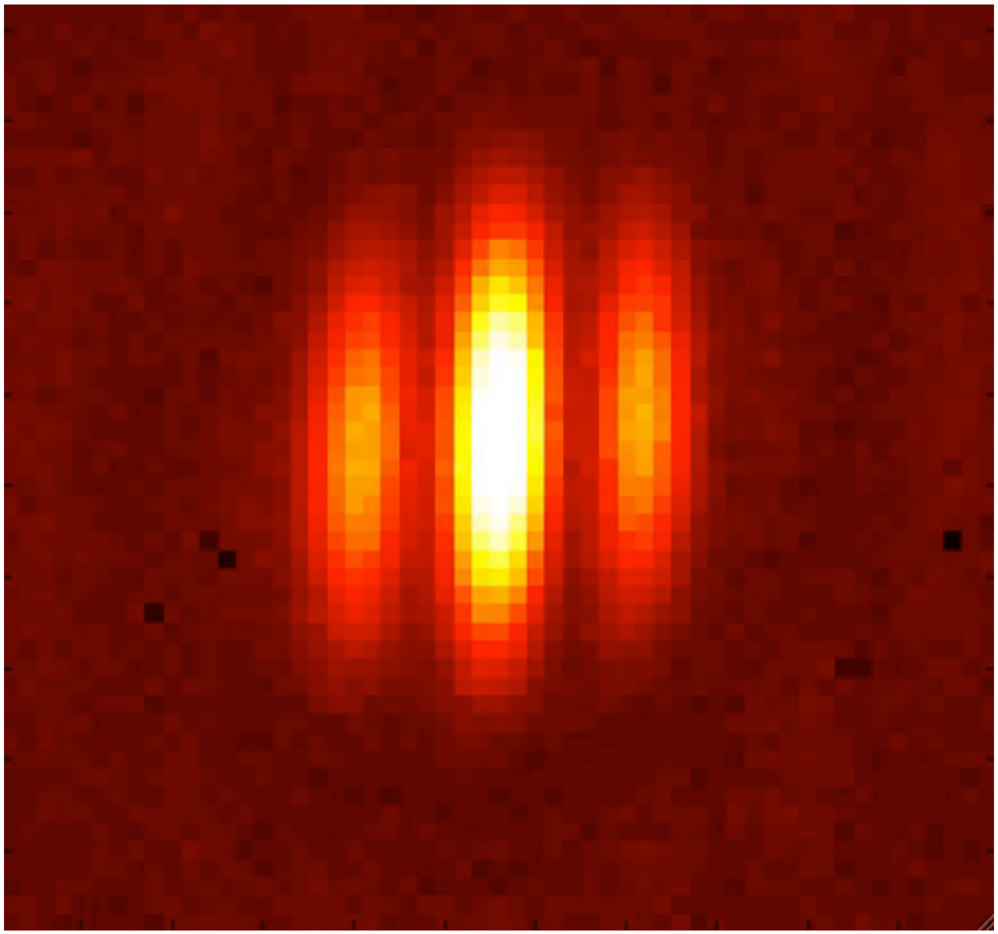

1 arcsec

Visible seeing was 1.6”

Each
image is 0.25 s

Phase variations from atmosphere.

LMIRCam Imaging

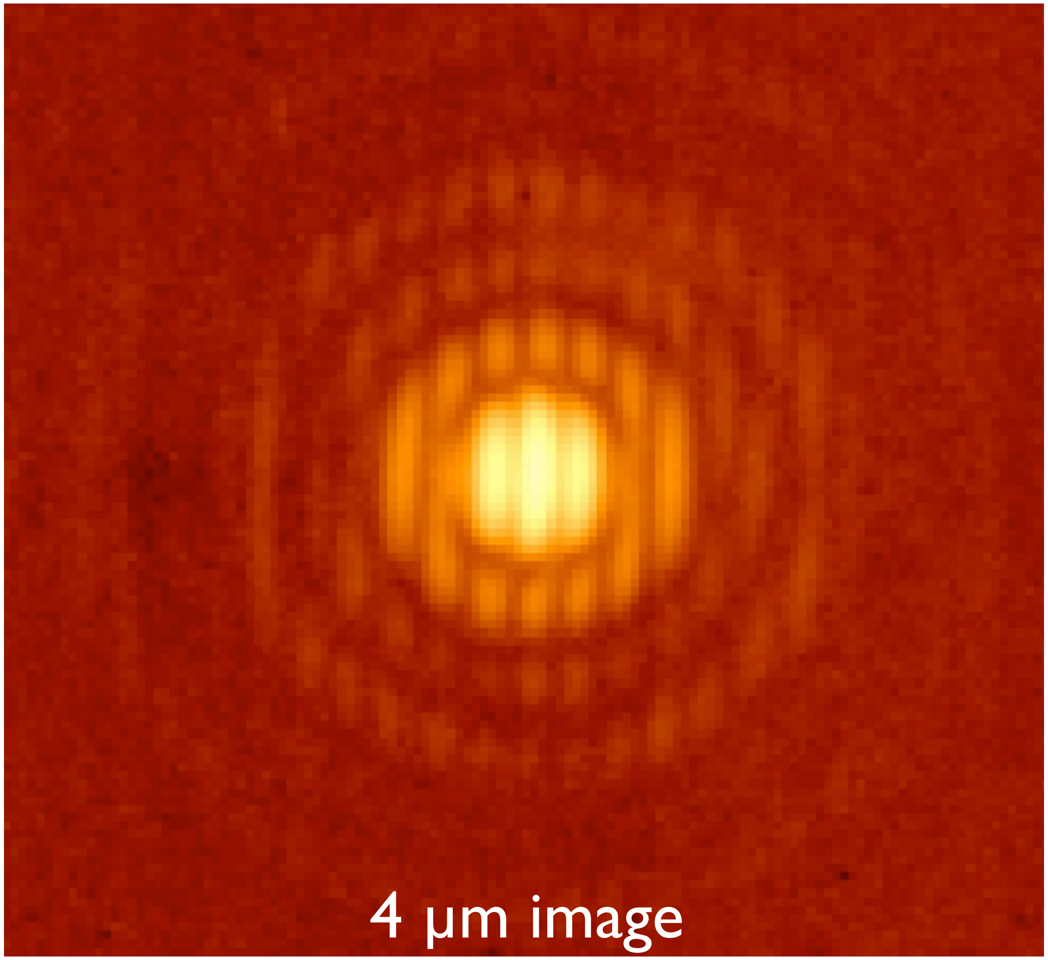

V=0.65

Best 5% of LMIRCam images in a sequence.

CH Cyg and calibrator

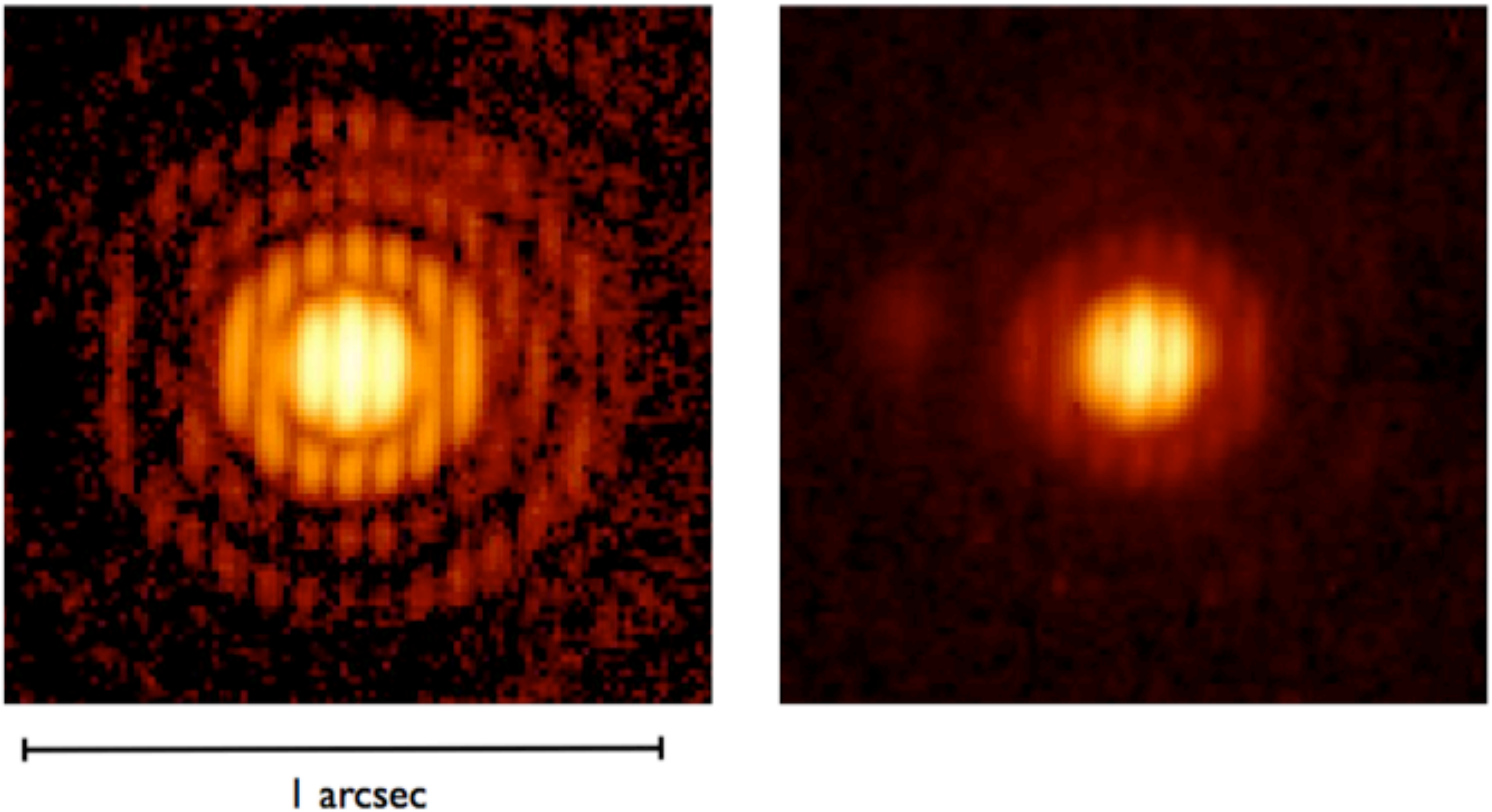

Co-axial beam combination: Temporal scan of phase

Single measurement with a beam splitter does not provide sufficient information, as intensity, fringe visibility and phase (3 parameters) need to be measured.
Two approaches:

- more beam splitters, and phase shifts to sample sine wave on at least 4 points
- single beam splitter, but temporal known variation of phase: fringe scanning. The measurement is a fringe packet

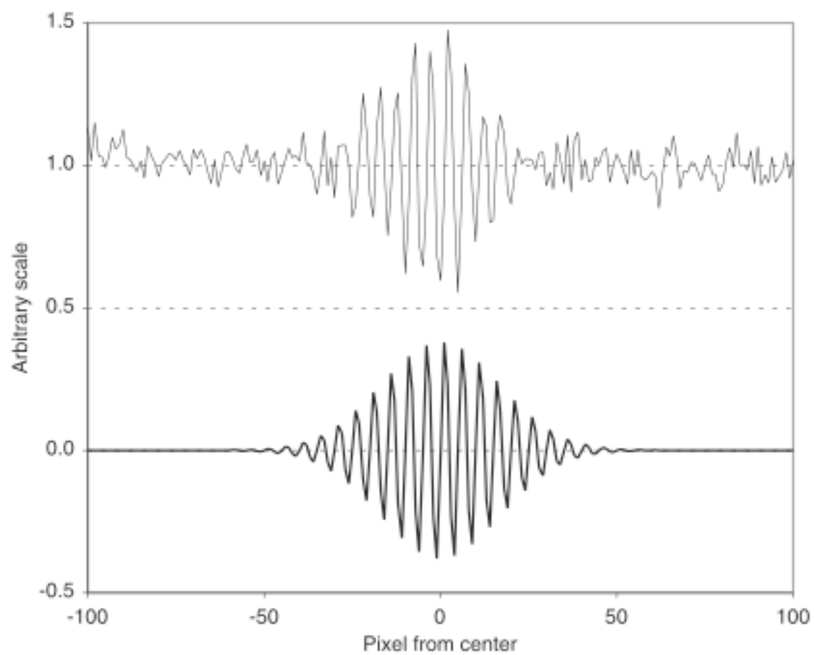

Fringe packet width is limited by coherence length

x axis: time, OPD

Combining beams with beam splitters

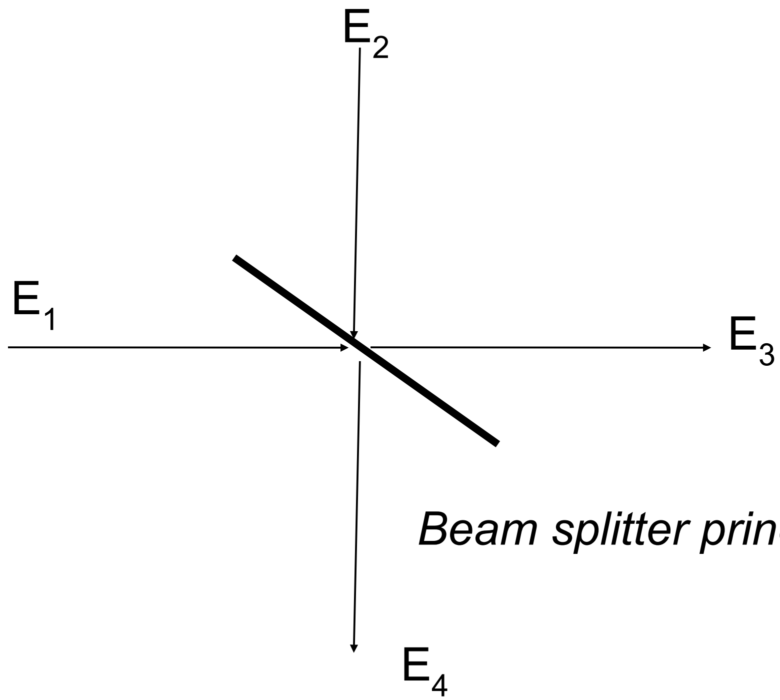

Beam splitter principle

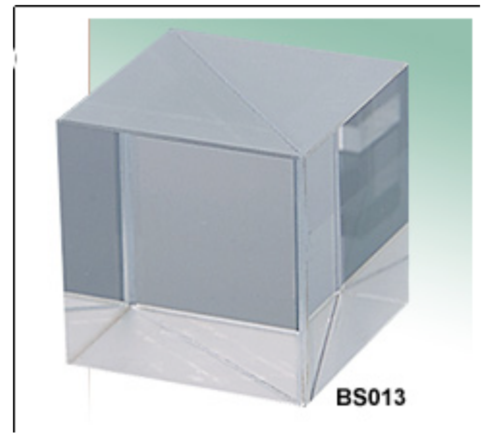

output
(complex numbers)

input
(complex numbers)

$$\begin{matrix} E_3 \\ E_4 \end{matrix} = \boxed{\begin{matrix} T_{31} & R_{32} \\ R_{41} & T_{42} \end{matrix}} \begin{matrix} E_1 \\ E_2 \end{matrix}$$

beam splitter matrix
Unitary matrix (conserves flux)

$T_{31} = T_{42} = T = |T|e^{i\phi t}$
$R_{32} = R_{41} = R = |R|e^{i\phi r}$

$R^2 + T^2 = 1$

$|\phi r - \phi t| = \pi/2$

For 50/50 beam splitter:
$|R| = |T| = 1/\text{sqrt}(2)$

Coaxial Observations

Measure fringe at 4 points over one wavelength of OPD (or derive these values from a fit).

Then if:

X=A-C

Y=B-D

N=A+B+C+D

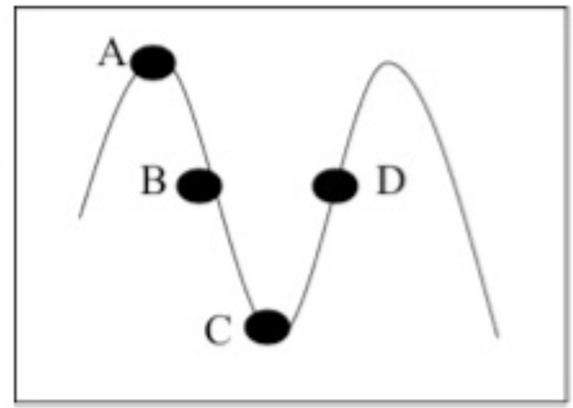

$$V^2 = \frac{\pi^2}{2} \frac{X^2 + Y^2}{N^2}$$

$$tan\phi = \frac{Y}{X}$$

See Colavita 1999 for discussion of data analysis.

Combining beams with single-mode optical fibers

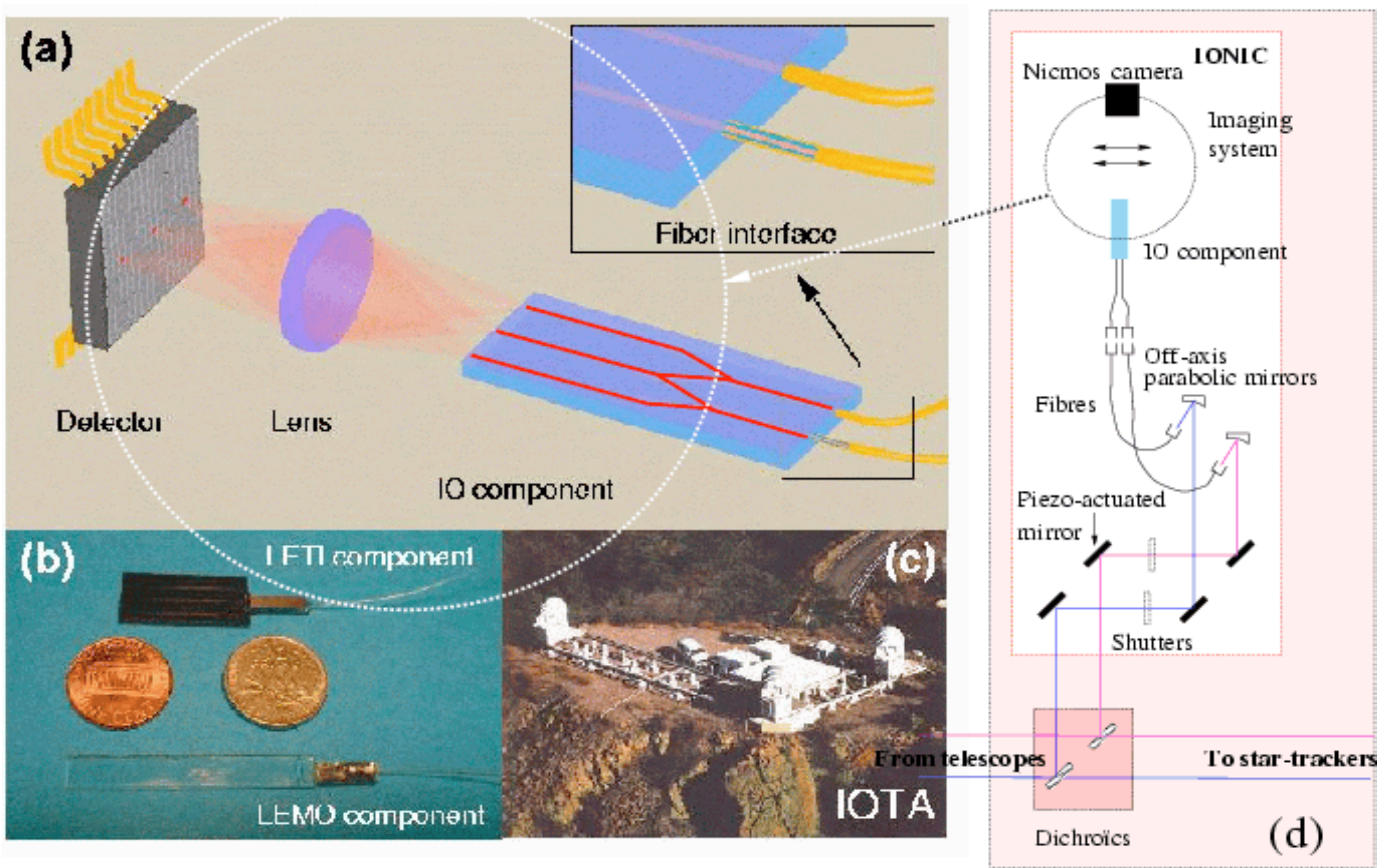

IOTA interferometer near-IR 2-beam integrated optics beam combiner (Berger et al. 2001)

Fiber beam combiner in integrated optics

This slide shows how photometric outputs are used to calibrate interferometric fringes in an interferometer

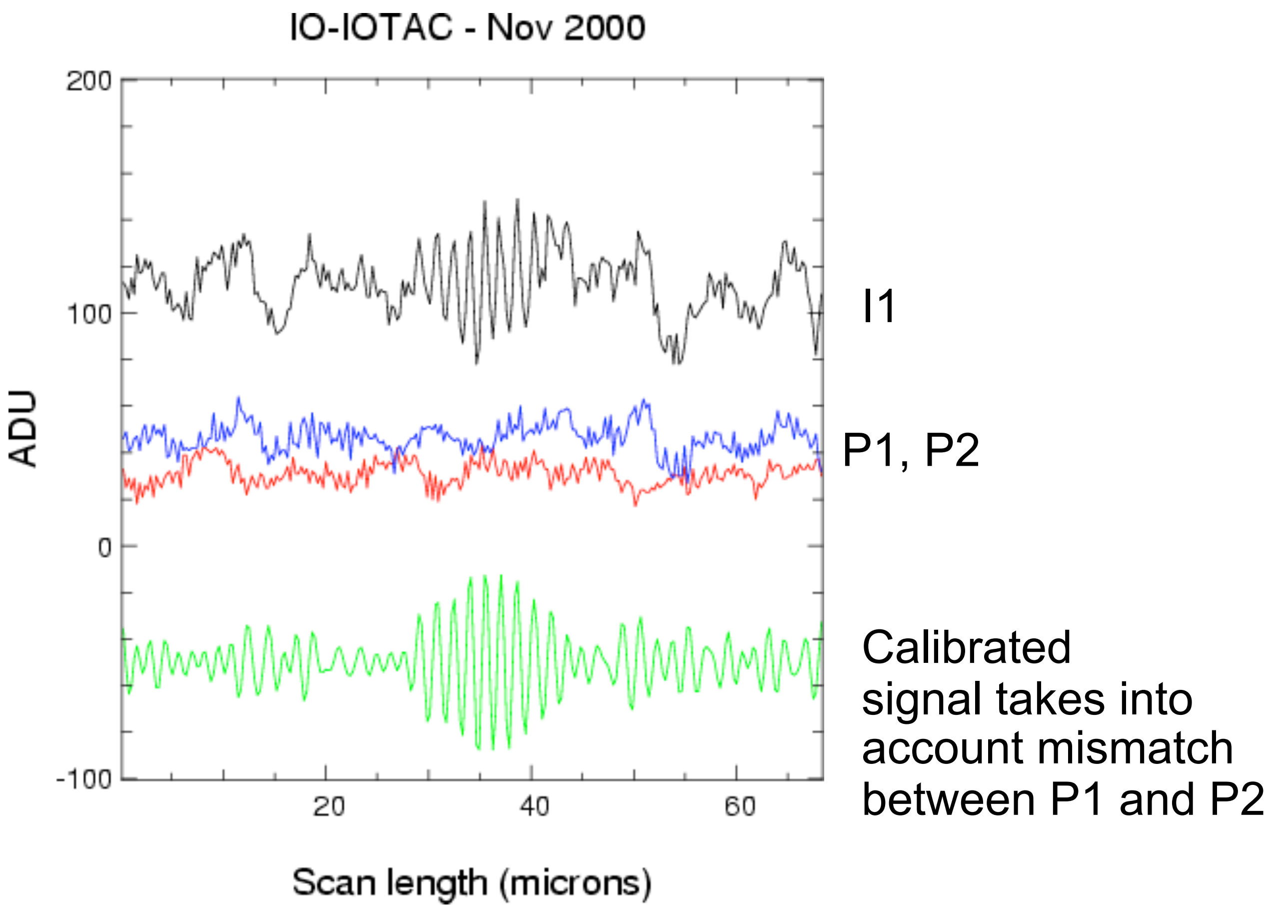

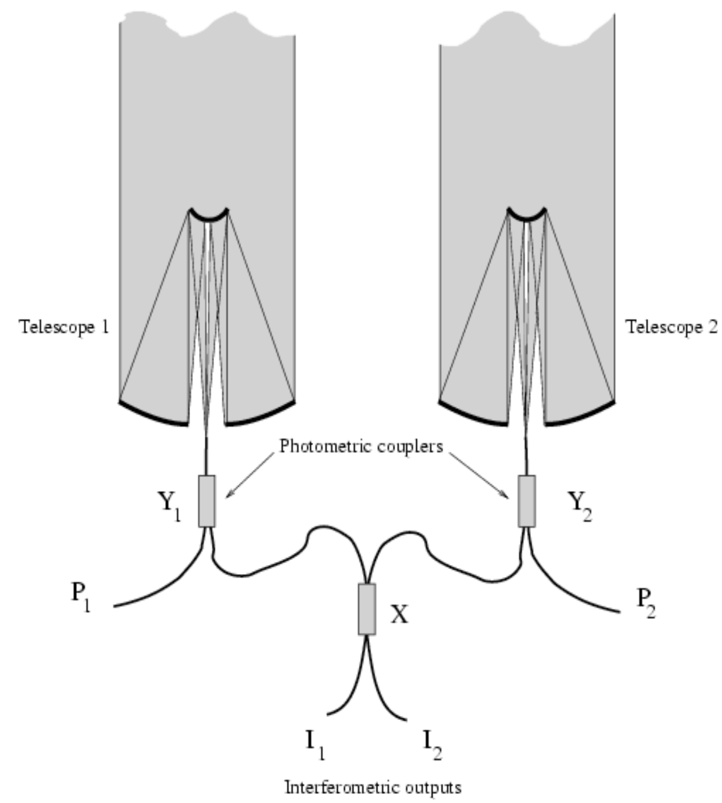

IOTA fiber interferometer (Berger et al. 2001)

Fiber combiners can enable compact instruments thanks to integrated optics

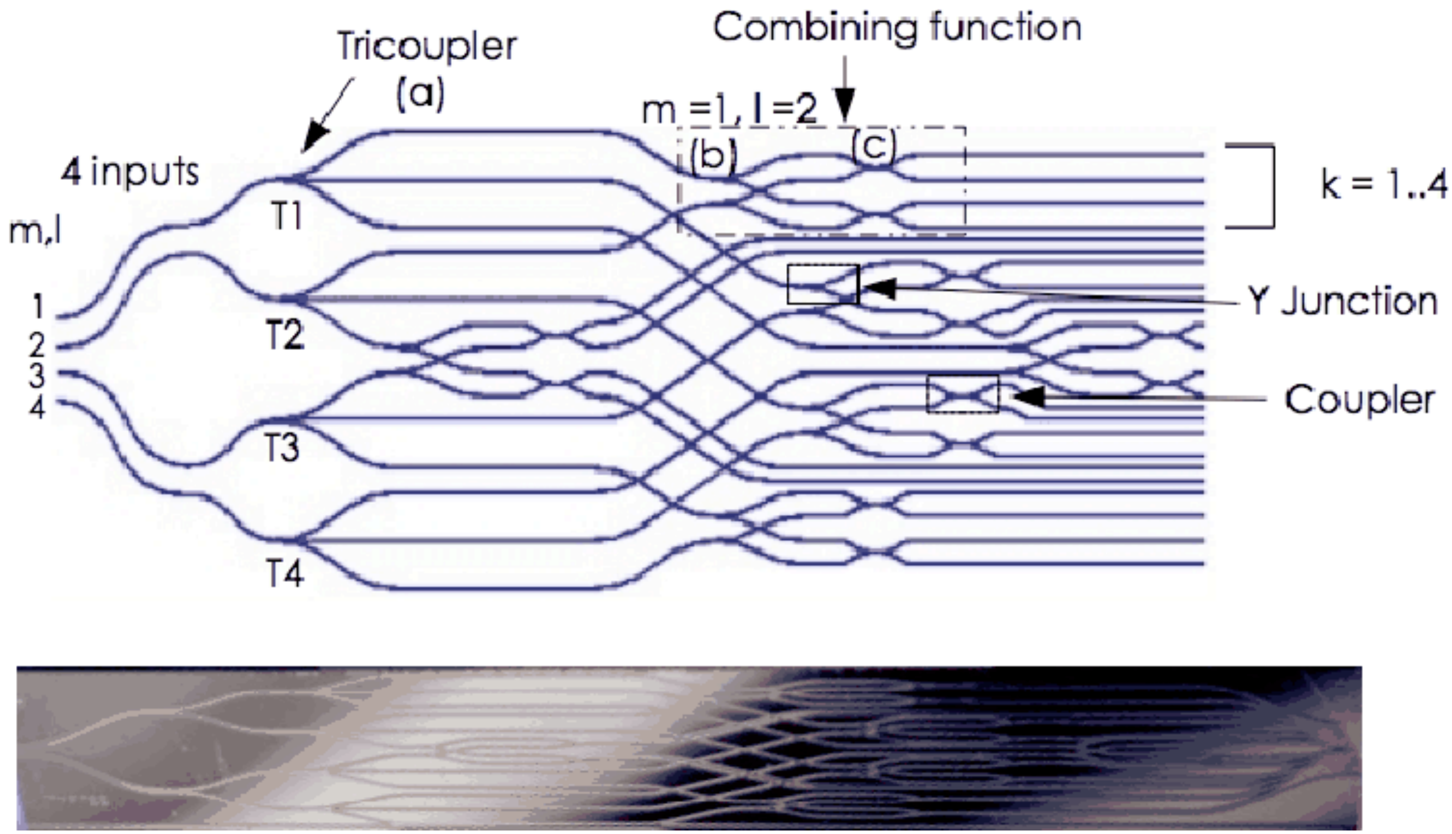

Prototype near-IR 4-beam combiner (Benisty et al. 2009)

Multi (N>2) telescopes interferometry: why >2 telescopes ?

Number of independent measurements increases rapidly with N:

Number of baselines for an interferometer with N apertures = N(N-1)/2
→ 2x more apertures ~ 4x more baselines

Since the number of measurements increases faster than the number of apertures, with large N, it becomes possible to calibrate out measurement errors with **phase closures** (discussed in next lecture)

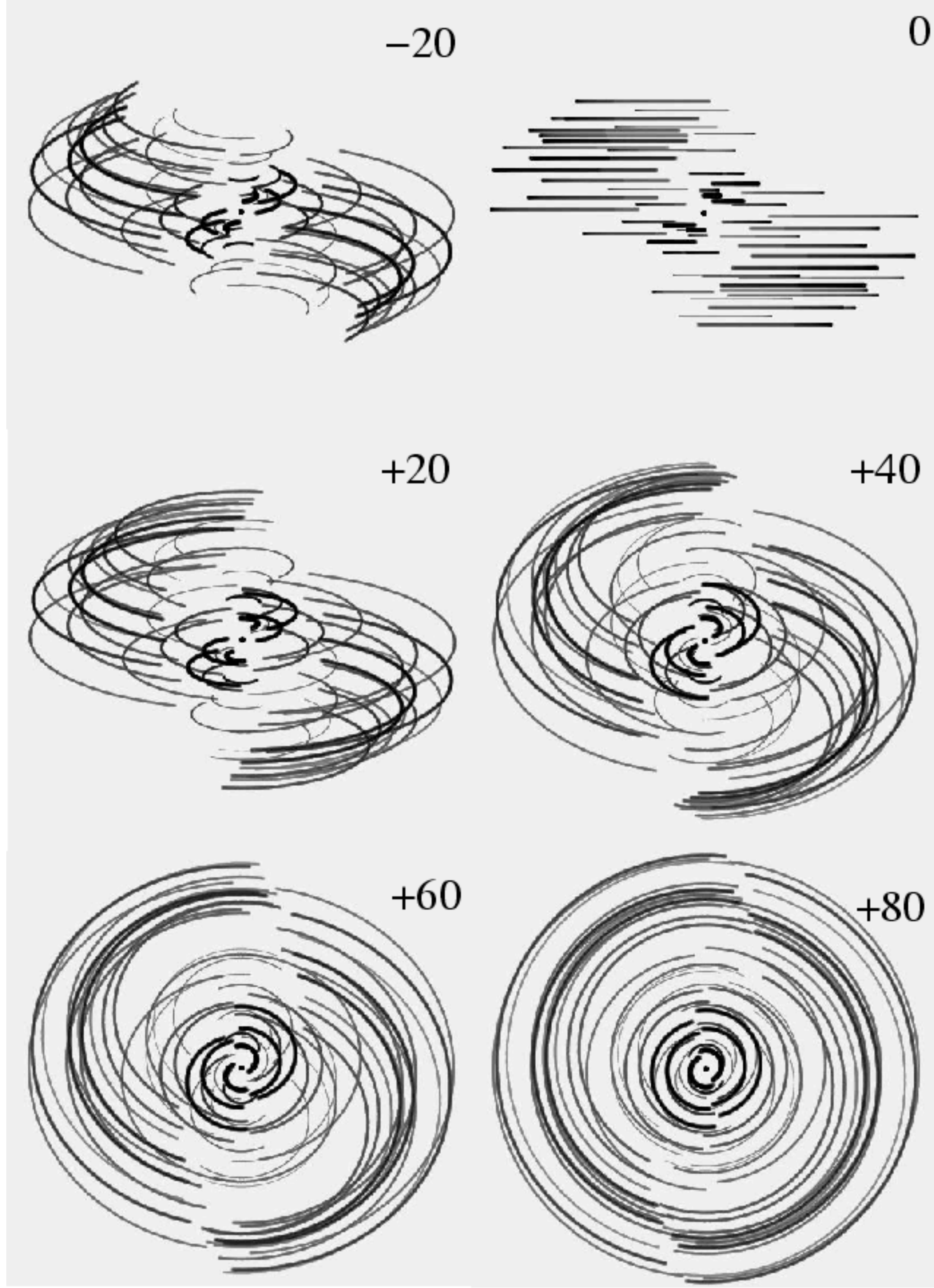

Simulated (u,v) plane coverage for telescopes atop Mauna Kea, as a function of source DEC

VLTI u-v plane coverage

The uv-plane

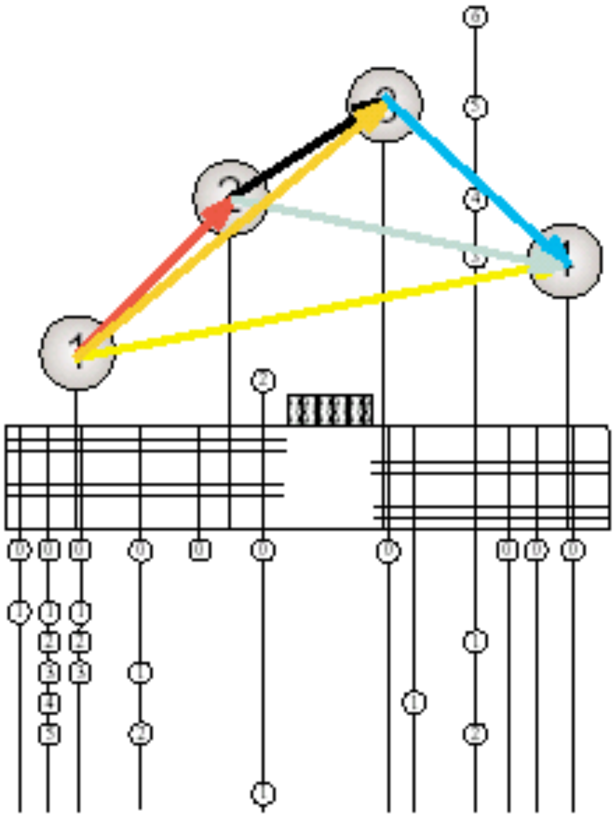

This is the uv-plane:

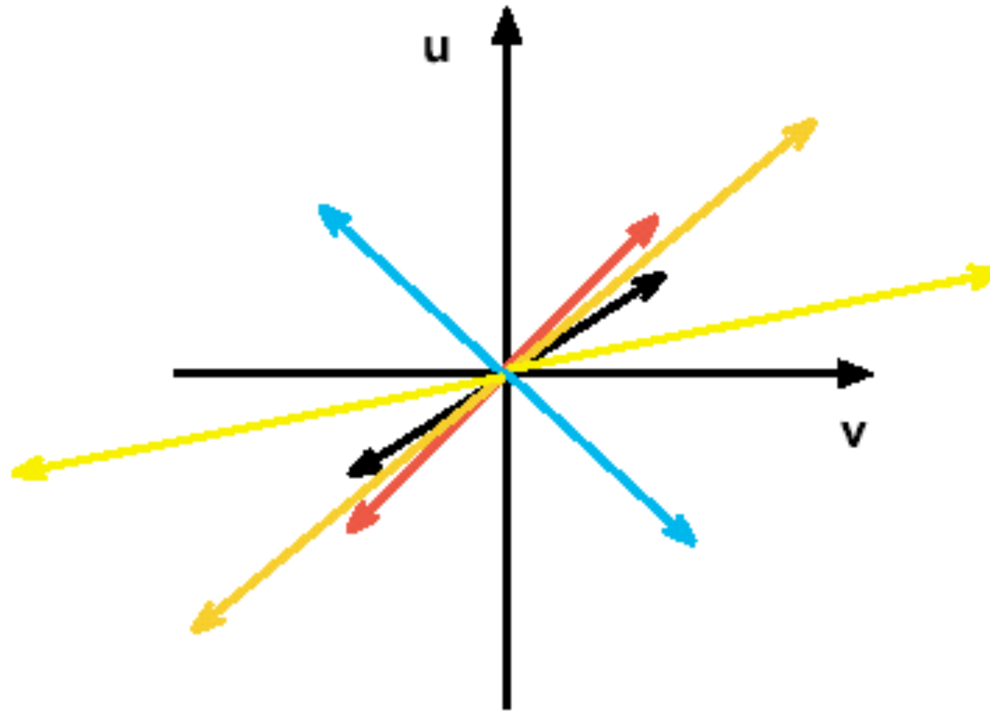

Note: This is the uv-plane for an object at zenith.
In general, the projected baselines have to be used.

VLTI u-v plane coverage

The uv-plane with the UTs

uv coverage for object at -15°

8 hour observation with all UTs

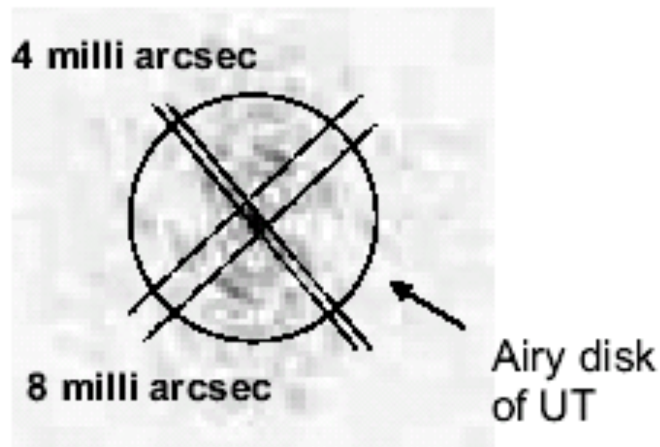

Resulting PSF is the Fourier transform of the visibilities

$\lambda = 2.2\mu m$ (K-band)

Need to measure visibility and phase to synthesize image.

VLT interferometer: 4 large 8m telescopes + smaller 1.8m auxiliary telescopes

CHARA array: six 1-m telescopes (Mt Wilson, USA)

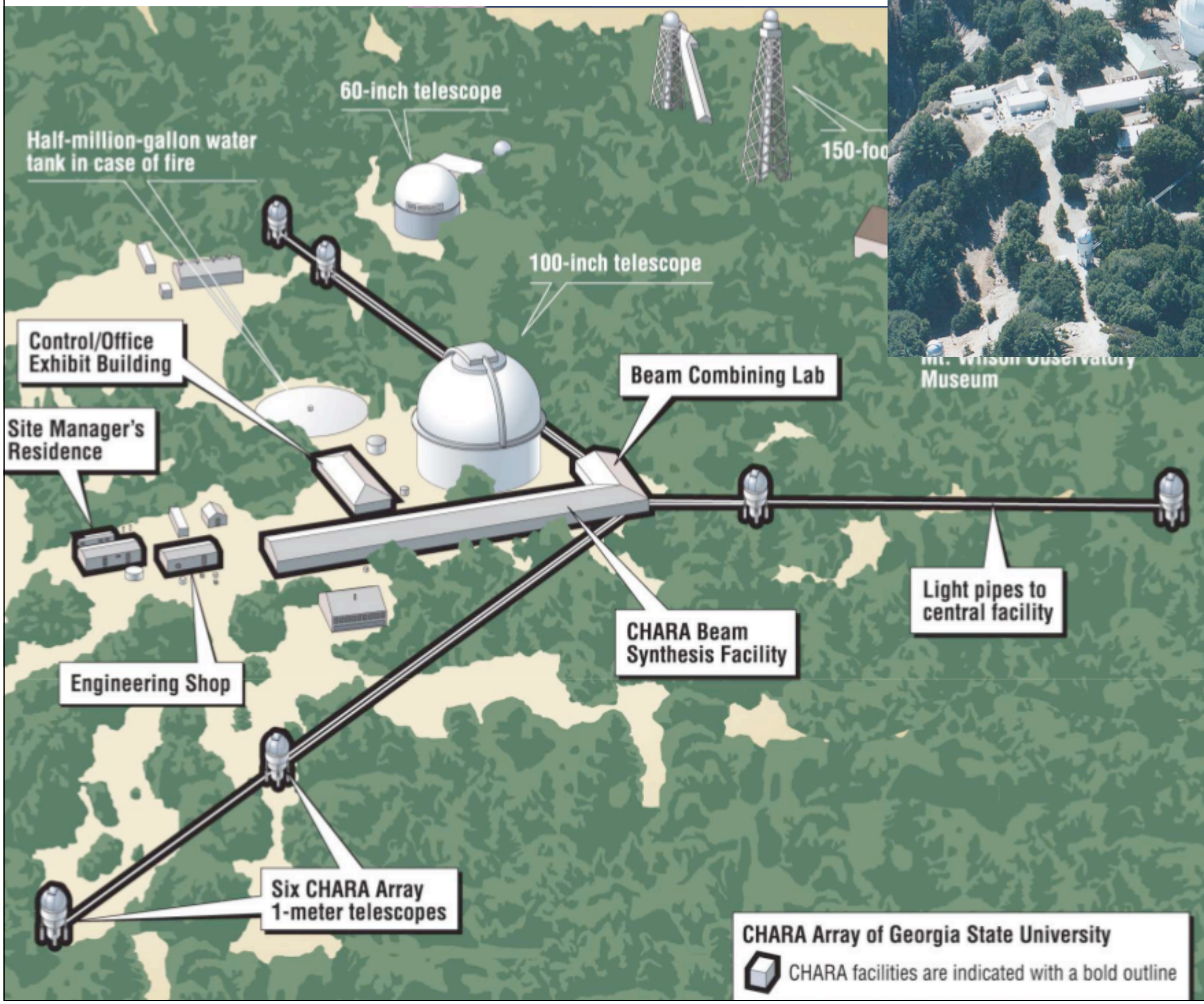

CHARA image of Altair

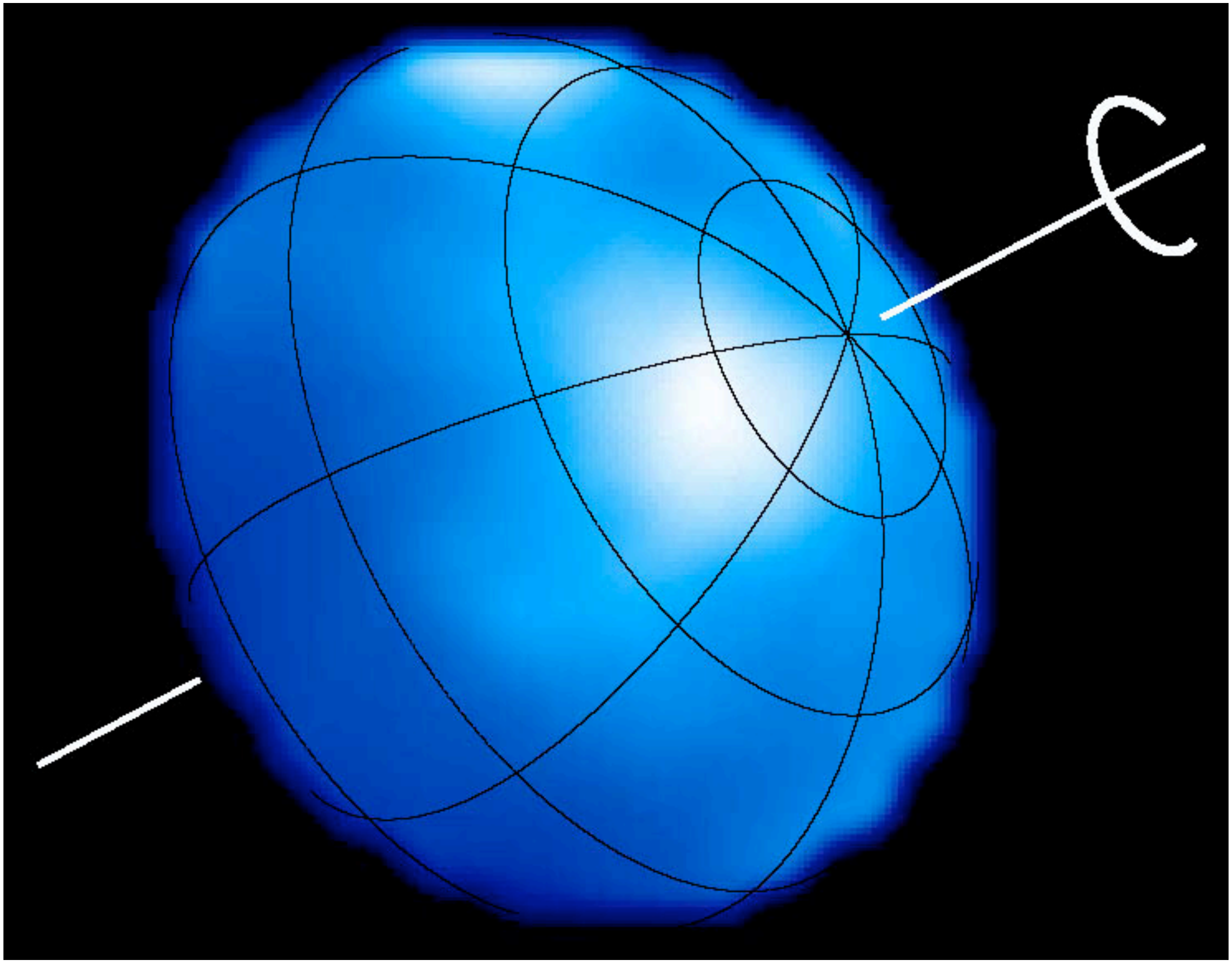

CHARA image of Epsilon Aurigae

Large number of apertures (6) + Earth's rotation allow sufficient uv plane coverage to reconstruct images of complex sources.
Epsilon Auriga is a bright naked eye star periodically eclipsed by a disk-bearing companion.

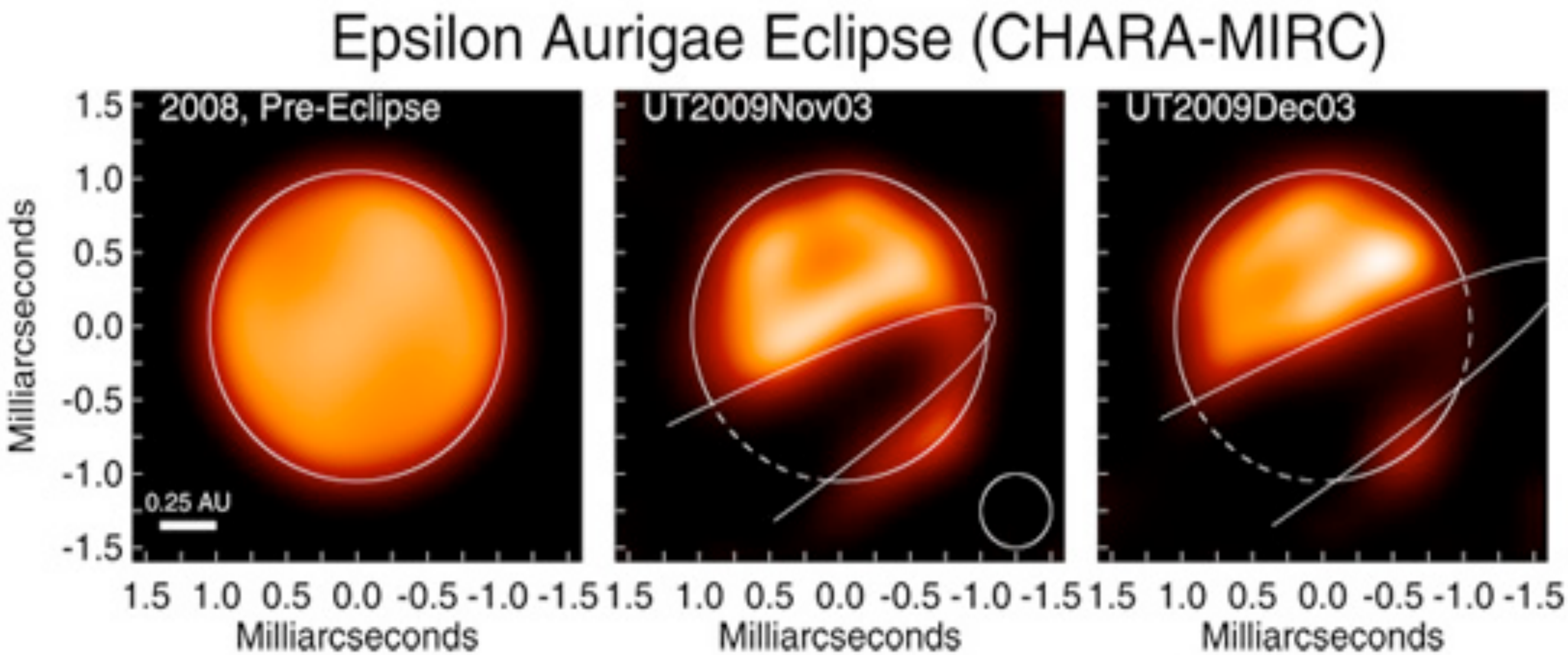

Flux limitation in interferometers

Throughput in an interferometer is often low, due to large number of optical elements:
telescope, beam transport, delay lines, beam combiner

Atmospheric turbulence and vibrations move fringes very rapidly
Measurement is only possible if individual exposure time << time it takes for fringe to move by a wavelength

With no phase tracking, difficult to observe faint targets

Typical limiting magnitudes for interferometers: 5 to 10 in visible / near-IR

To extend this limit, need to be able to track and lock fringes to allow long exposures
this will be discussed in next lecture

Brightness Estimation

Observations typically requires 100-1000 Hz sampling to “freeze” the seeing.

Consider fringe sensing carried out in K band (2.0-2.4 microns):

an 8 m aperture receives ~15,000 photons from a K=10 star in 1 ms.

sky background is ~1500 photons/ms.

Telescope background is ~15,000 photons/ms.

throughput is 6%.

This gives an SNR of 8 in a 1 ms exposure.

Astrometric precision of measurement:

$$\delta x = \lambda / B \; 1 / SNR$$

Phase & amplitude correction and calibration in interferometers

OUTLINE:

Phase referencing in interferometers

- why phase referencing? beyond V^2 interferometry: astrometry, image synthesis, phase closure

Wavefront correction on individual apertures
tradeoff between calibration accuracy, efficiency and wavefront quality

Technology:

- delay lines
- atmospheric dispersion compensation: vacuum delay lines, ADCs
- Adaptive optics correction in interferometers
- Calibration of residual phase errors with spatial filtering: pinhole, fiber interferometry

Delay lines

Must maintain near-zero Optical Pathlength Difference (OPD) between arms of the interferometer

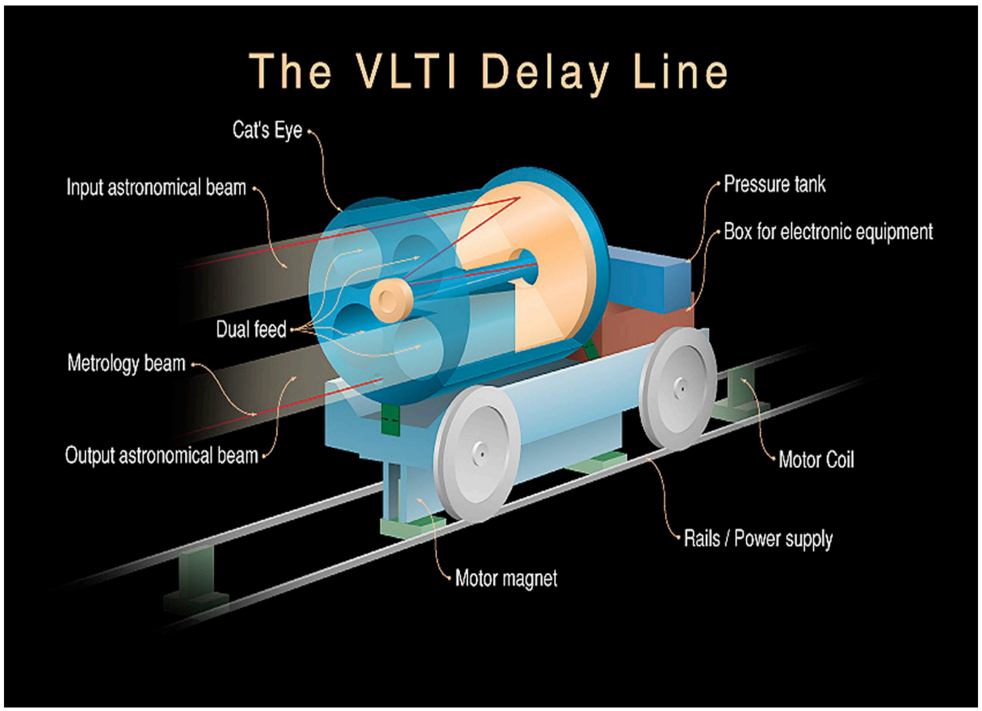

VLTI delay line moving cart

Keck interferometer coarse delay lines

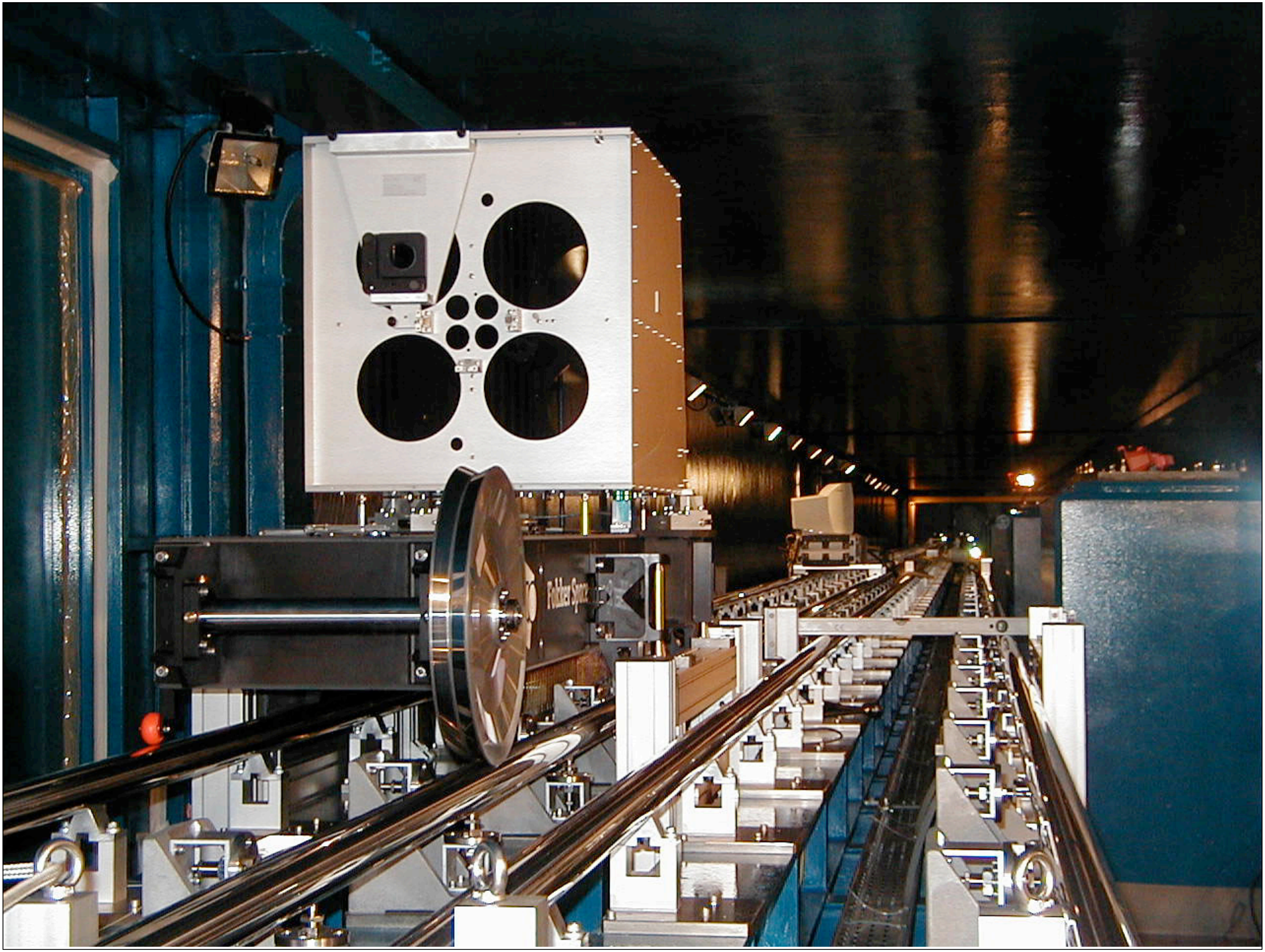
Fokker Space

Part 1:
Control and calibration of visibility in interferometers

Scientific motivation

Why is fringe visibility accuracy important ?

$$V^2(B\theta/\lambda) = \left(2\frac{J_1(\pi B\theta/\lambda)}{\pi B\theta/\lambda}\right)^2$$

Example below shows effect of fringe visibility measurement accuracy on measurement of stellar diameters (in this example, used to measure absolute distance to Cepheid stars)

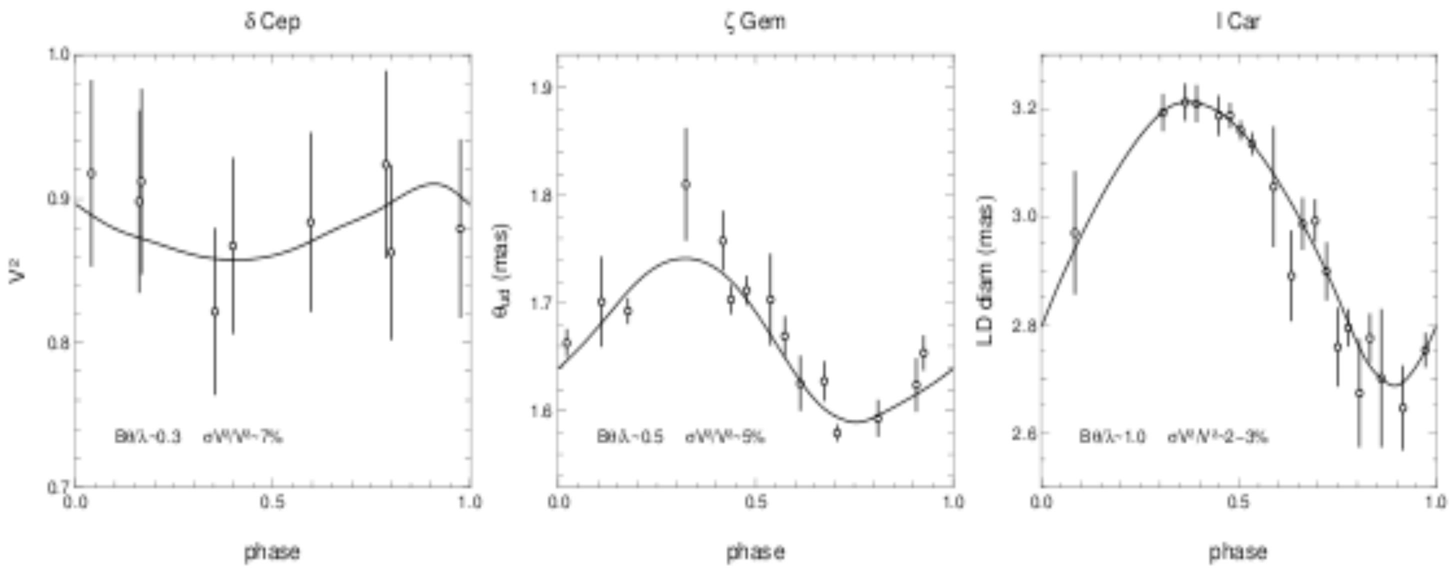

Figure 1. Different interferometric attempts to measure Cepheid angular diameter variations. From left to right: Mourard et al. (1997[6]), Lane et al. (2000[7]) and Kervella et al. (2004[8]). The left panel is V^2 as a function of phase, while the panels to the right are angular diameters with respect to phase. The thin, continuous line is the integration of the pulsation velocity (distance has been adjusted). From left to right, one can see the effect of increasing resolution ($B\theta/\lambda$) and improving precision ($\sigma V^2/V^2$). In the left panel, the pulsation was not claimed to be detected; the middle panel was the first detection, with a 10% precision on the distance; the right panel displays one of the best: 4% in the distance.

A. Merand, Cepheids at high angular resolution

Sources of fringe visibility loss (discussed in next slides)

What can go wrong ? Why would the measured fringe visibility be < 1 on a point source ?

Amplitude difference between the 2 beams
Problem: If one beam is brighter than the other, fringe visibility <1
→ measure flux in each arm of the interferometer

Phase errors within each of the 2 beams
Problem: Wavefront is not flat before entering the beam combiner
→ calibrate visibility loss by observing another star
→ good adaptive optics for each of the telescopes
→ spatial filtering to clean the beams, at the cost of flux

Phase between the 2 beams is changing within detector exposure time
Problem: Measurement is superposition of shifted fringes, with apparent V < 1
→ calibrate visibility loss by observing another star
→ reduce / calibrate internal sources of vibration
→ if possible, fringe tracking on nearby bright source

Phase between the 2 beams is changing within the spectral band of the measurement
Problem: Dispersion in atmosphere and interferometer: measurement is superposition of shifted fringes, with apparent V < 1
→ optically compensate atmospheric dispersion
→ calibrate visibility loss by observing another star
→ disperse fringes on detector
→ use vacuum delay lines

Polarization is different between the 2 beams
Problem: internal instrumental polarization in interferometer
→ calibrate visibility loss by observing another star
→ design telescopes, beam transport and delay lines to minimize differential polarization effects

Fringe visibility loss: phase errors in beams

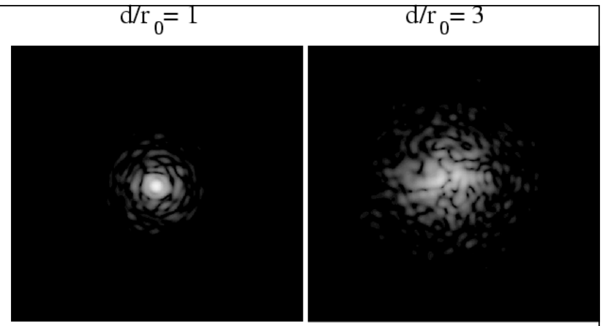

Example:
2 beams are combined with a beam splitter
Each beam has phase errors, and differential phase error between the beams is ~1 rad
consider 3 points in the pupil:

- point 1: phase difference between 2 beams is -1 rad
- point 2: phase difference between 2 beams is 0 rad
- point 3: phase difference between 2 beams is +1 rad

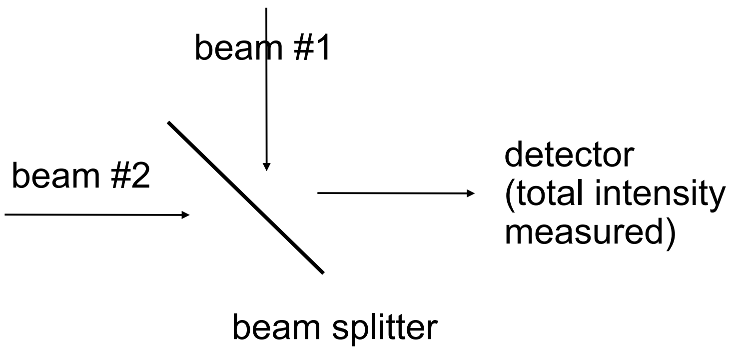

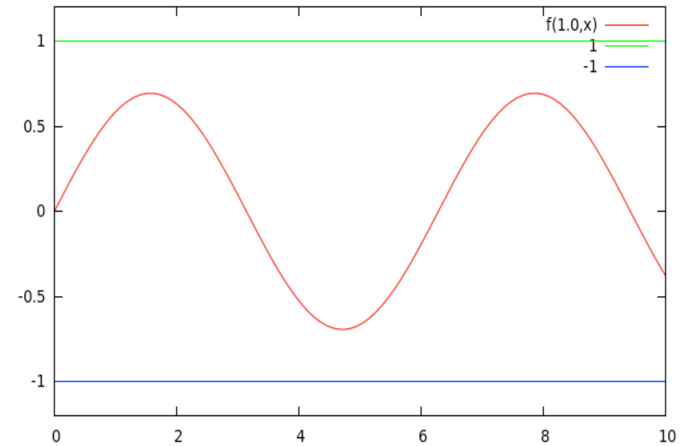

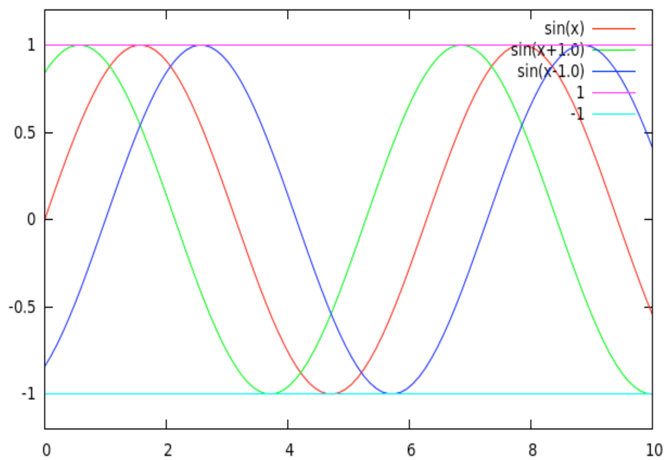

for each of the 3 points, visibility is = 1, but phase is offset

What is observed is the total flux, the sum of the 3 curves on the left
Measured visibility = 0.7 < 1.0
problem:
Is measured visibility due to aberrations, or true object visibility

Same concept applies to variations of phase with time and wavelength

Fringe visibility loss: phase errors in beams
Solutions to problem

Visibility loss is approximately equal to Strehl ratio ~ $\exp(-\sigma^2)$
With σ = 1 radian RMS, visibility ~ 0.3

Good **adaptive optics correction** to reduce σ is essential on large telescopes

Spatial filtering can be used to clean beam:
Optically transforms aberrated wavefront into flat wavefront
With aberrated wavefront, light is lost by spatial filtering

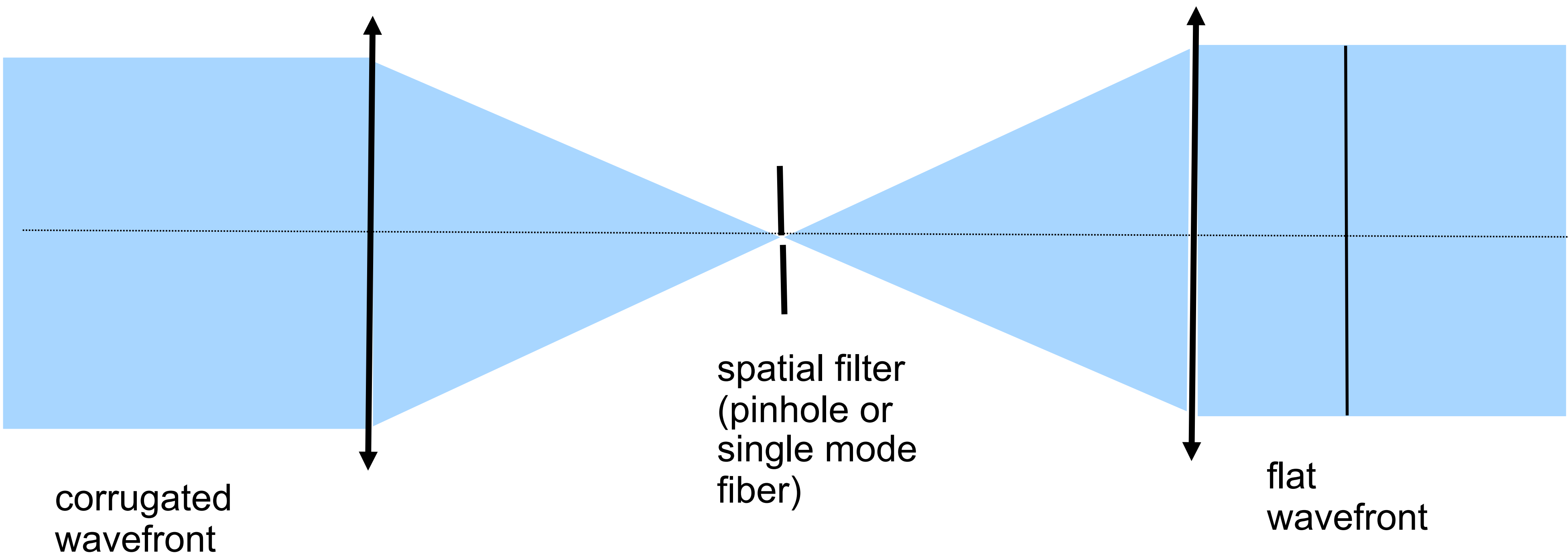

Spatial filtering

Spatial filtering alone does not help, as flux variations in interferometer arms are strong

Photometric calibration, achieved by measuring light in both arms of the interferometer AFTER spatial filtering, can calibrate visibility loss due to flux variations.

Spatial filtering + photometric calibration is powerful solution, and has achieved < % visibility accuracy on sky

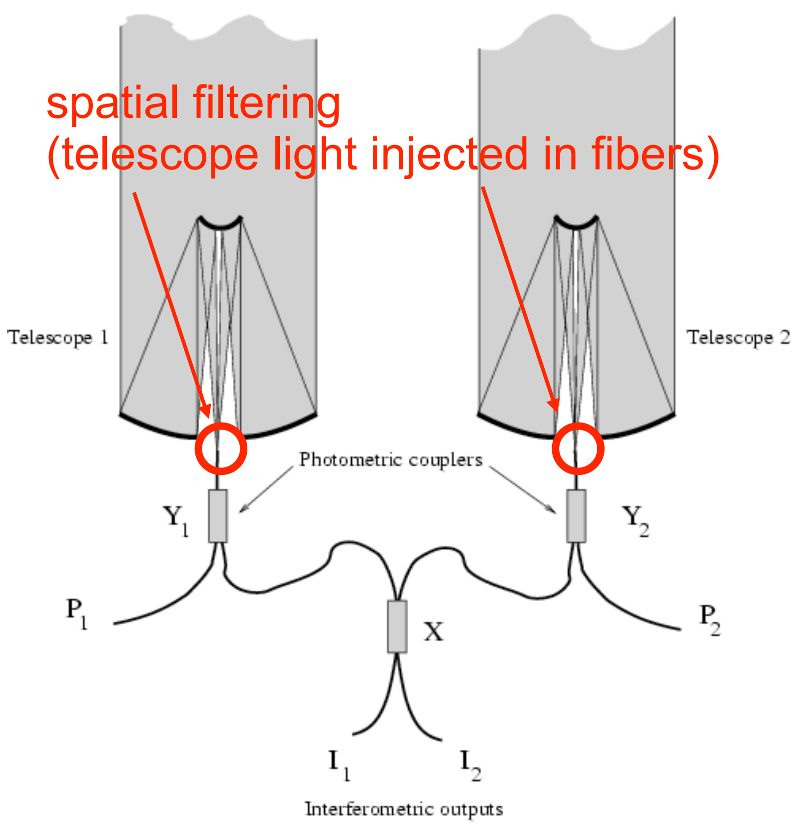

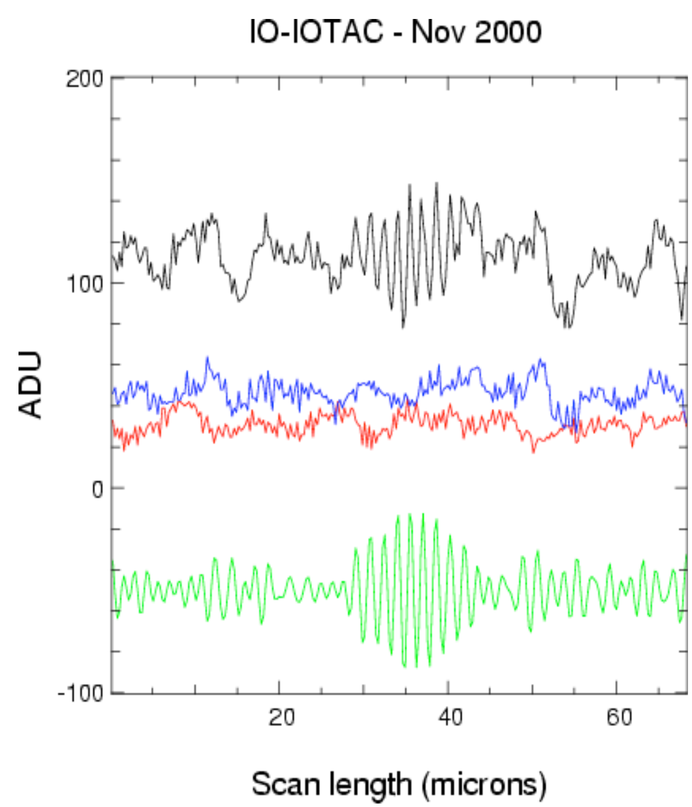

Uncalibrated signal: I_1

photometric channels: P_1, P_2

Calibrated signal takes into account mismatch between P1 and P2

IOTA fiber interferometer (Berger et al. 2001)

Fringe visibility loss: chromatic dispersion

Atmosphere introduces strong chromatic dispersion which needs to be compensated
In conventional interferometer, delay line introduces a delay (in air) to compensate for a vacuum delay → dispersion compensator is required.
Problem can be mitigated by using vacuum delay lines

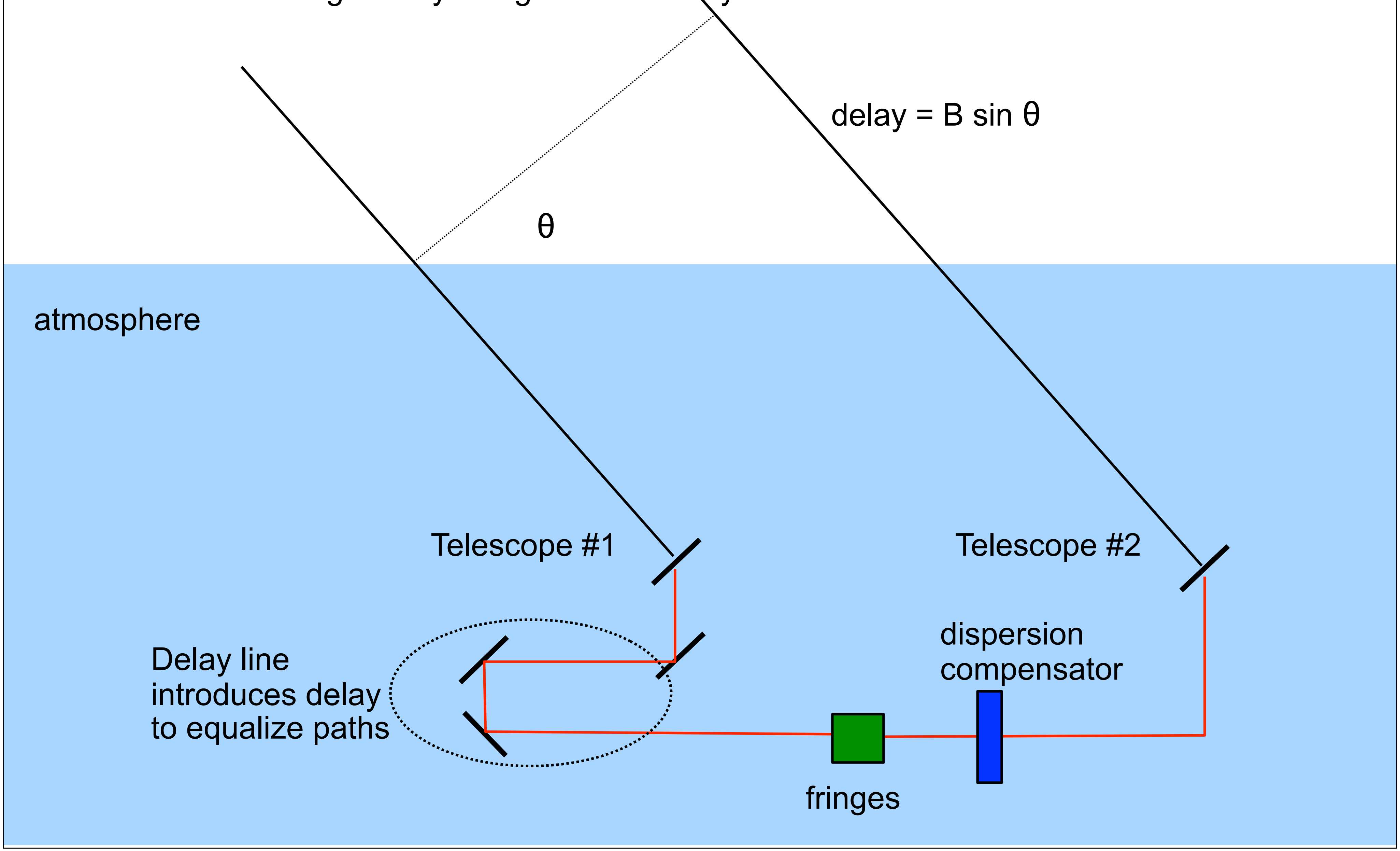

Vacuum delay lines (CHARA interferometer)

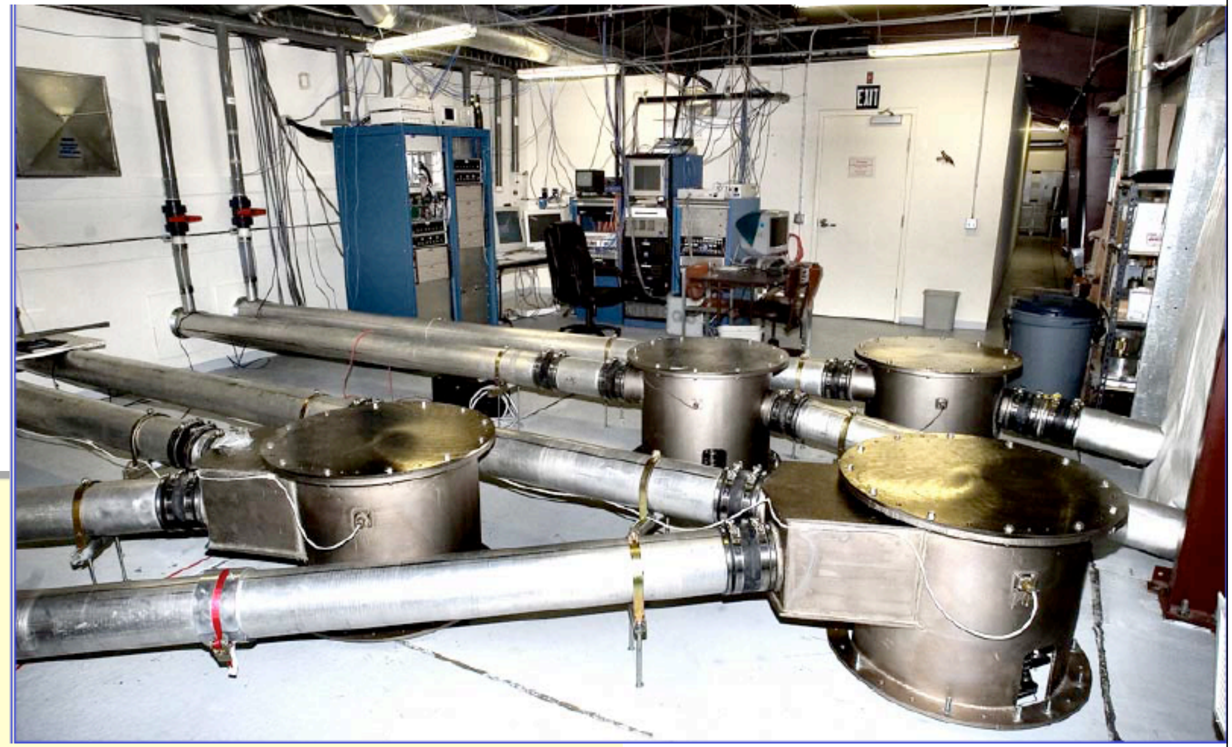

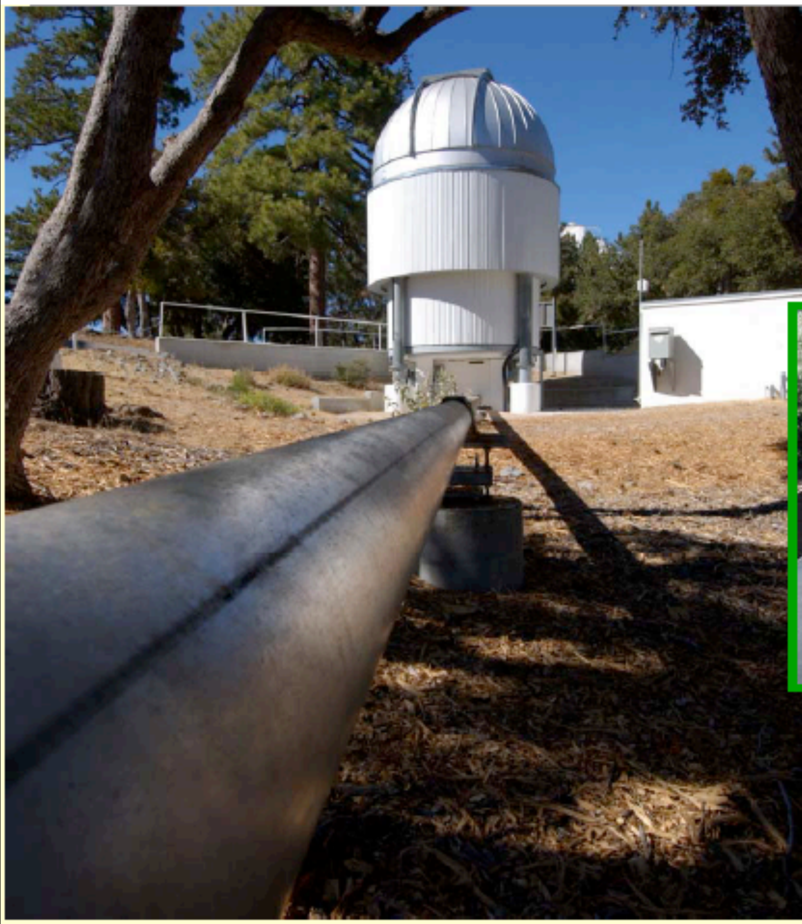

Part 2:
Control and calibration of fringe phases

Fringe tracking:
essential to allow observation of faint sources

Throughput in an interferometer is often low, due to large number of optical elements:
telescope, beam transport, delay lines, beam combiner

Atmospheric turbulence and vibrations move fringes very rapidly
Measurement is only possible if individual exposure time << time it takes for fringe to move by a wavelength → with no phase tracking, difficult to observe faint targets
Typical limiting magnitudes for interferometers: 5 to 10 in visible / near-IR
To extend this limit, one needs to track and lock fringes to allow long exposures

Observations typically requires 100-1000 Hz sampling to “freeze” the seeing.

Consider fringe sensing carried out in K band (2.0-2.4 microns):

an 8 m aperture receives ~15,000 photons from a K=10 star in 1 ms.

sky background is ~1500 photons/ms.

Telescope background is ~15,000 photons/ms.

throughput is 6%.

This gives an SNR of 8 in a 1 ms exposure.

Fringe tracking

Fringe tracker measures rapidly fringe position, and actively controls optical pathelength corrector (=fast delay line) at the input of the beam combiner

Enables longer exposures with the scientific instrument

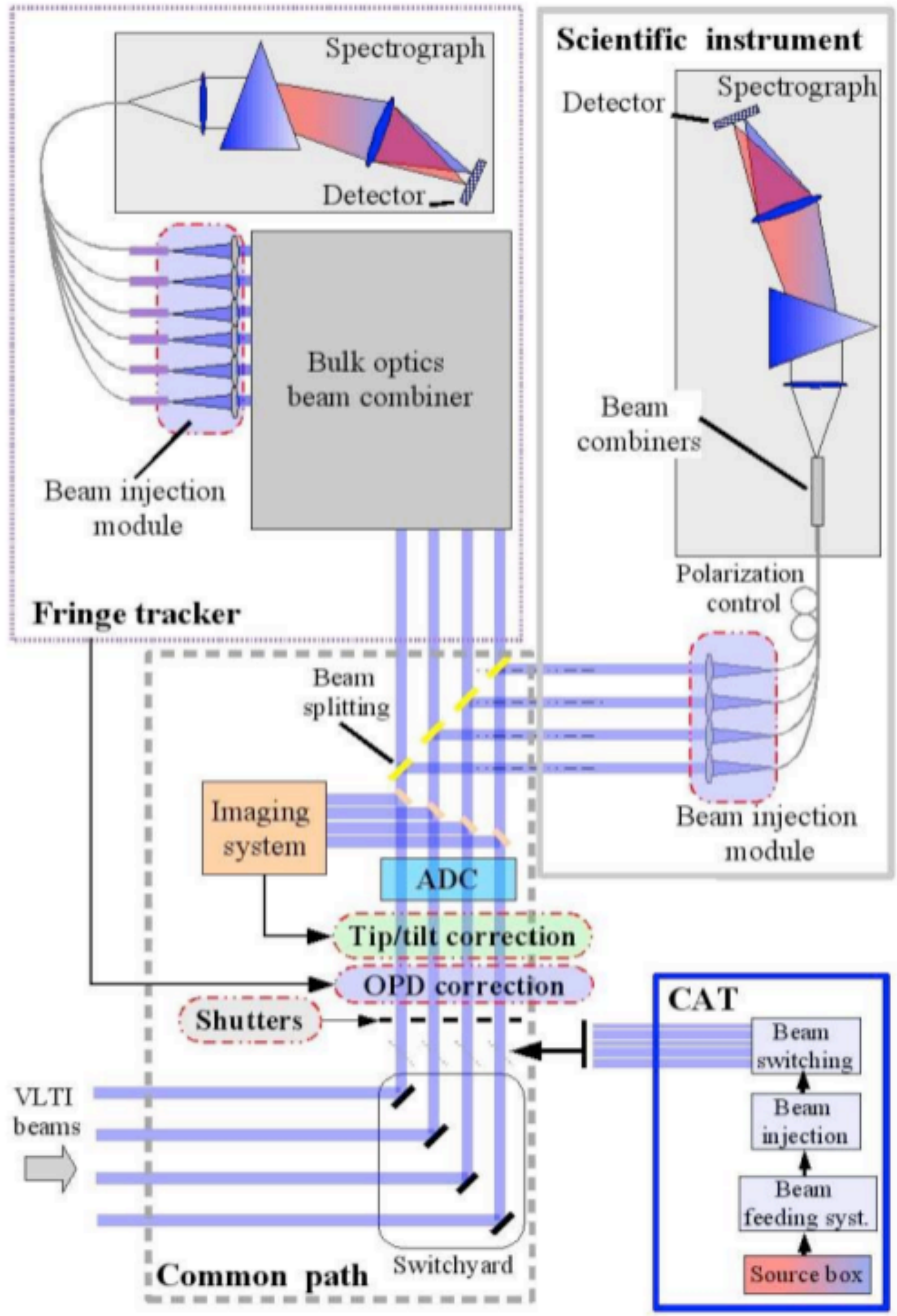

VLTI fringe tracker shown at the upper left corner of this figure (Corcione et al., 2008)

Phase referencing

Scientific motivations

Image reconstruction with multiple baselines requires measurement of phases and visibilities (with no phases, only centro-symmetric component of the image can be estimated)
Astrometric measurement (measuring position of sources) requires fringe phase
On a single baseline: astrometric error [rad] = phase error [rad] x (λ / 2π) / Baseline

How to reference phase ? - or what to use as a reference

A **nearby star** can be used to reference phase on a single baseline interferometer

Phase closure relationships can be used to separate instrumental phases from object phases (see next slides)

Phase can be measured as a function of wavelength:
object itself (at different wavelength) provides a reference
Example:
Accurately measuring photocenter as a function of wavelength with an interferometer can reveal planets, as hot planet is redder than star
See VLTI/Amber instrument for example

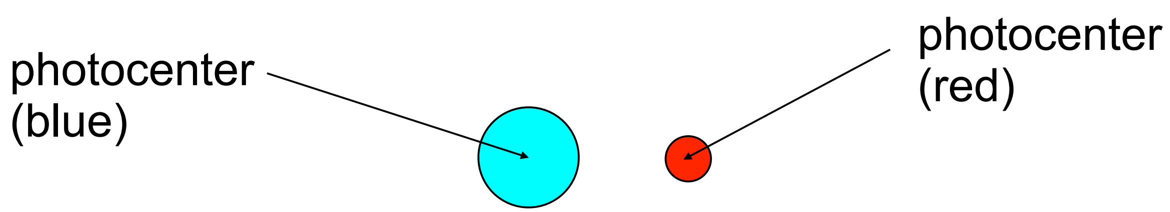

Phase closures

The fringe packet moves back and forth in an interferometer, due to phase changes that are caused by the atmosphere.

This variation causes the real phase to be unmeasurable for a single object.

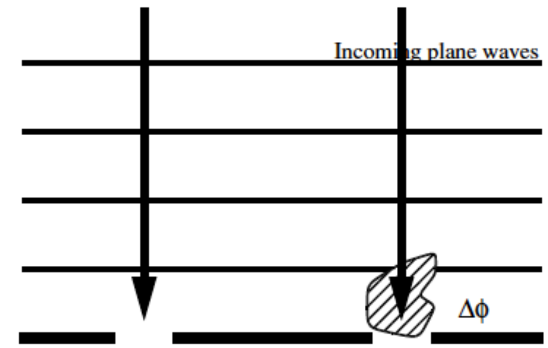

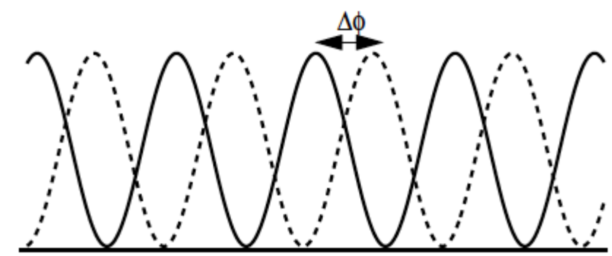

Individual phases change with atmospheric terms, alpha:

$$\phi_{12} = \theta_{12} + \alpha_1 - \alpha_2$$

$$\phi_{23} = \theta_{23} + \alpha_2 - \alpha_3$$

$$\phi_{31} = \theta_{31} + \alpha_3 - \alpha_1$$

Define a **closure phase** which gets rid of the atmosphere:

$$\Phi_{123} = \phi_{12} + \phi_{23} + \phi_{31} = \theta_{12} + \theta_{23} + \theta_{31}$$

There are (N-1)(N-2)/2 closure phases in an array.
3: 1 closure phase, 3 visibilities -> 33% of phase information recovered.
10: 36 closure phases, 45 visibilities -> 80% of phase information recovered.

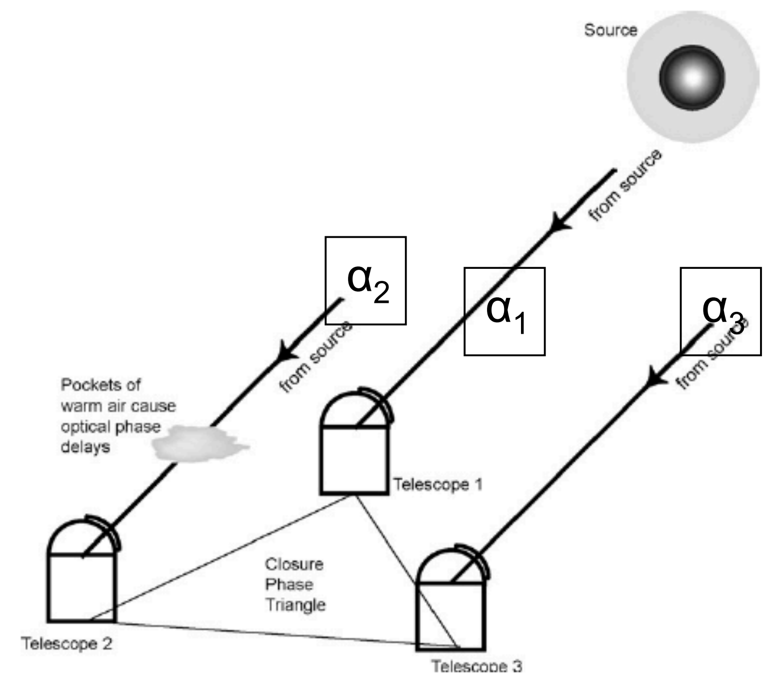

Fig. 4. Phase errors introduced at any telescope causes equal but opposite phase shifts in adjoining baselines, canceling out in the *closure phase* (see also Readhead et al., 1988; Monnier et al., 2006a).

Good Reference: Monnier 2007

Example 1 from Monnier 2007

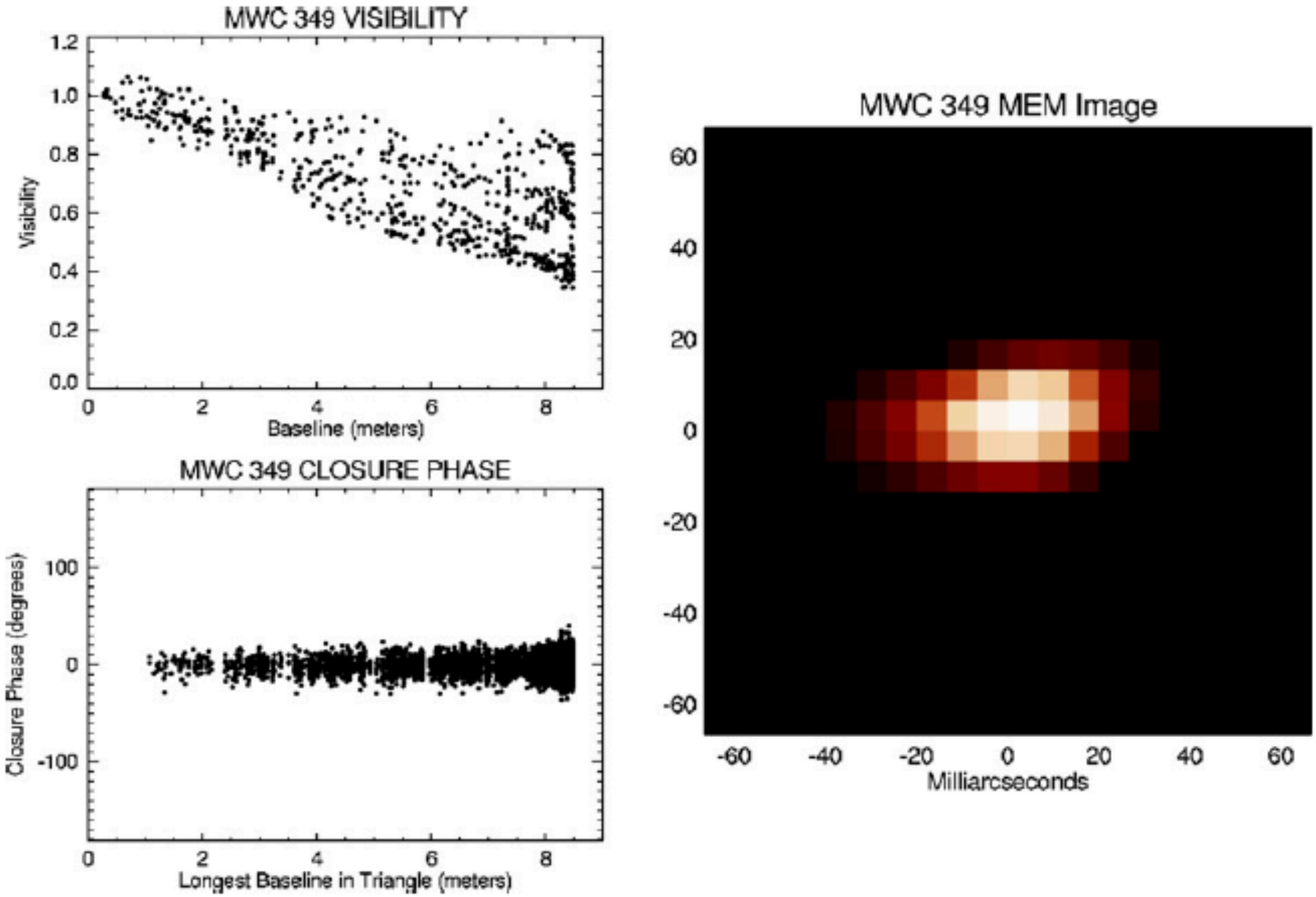

Example 2 from Monnier 2007

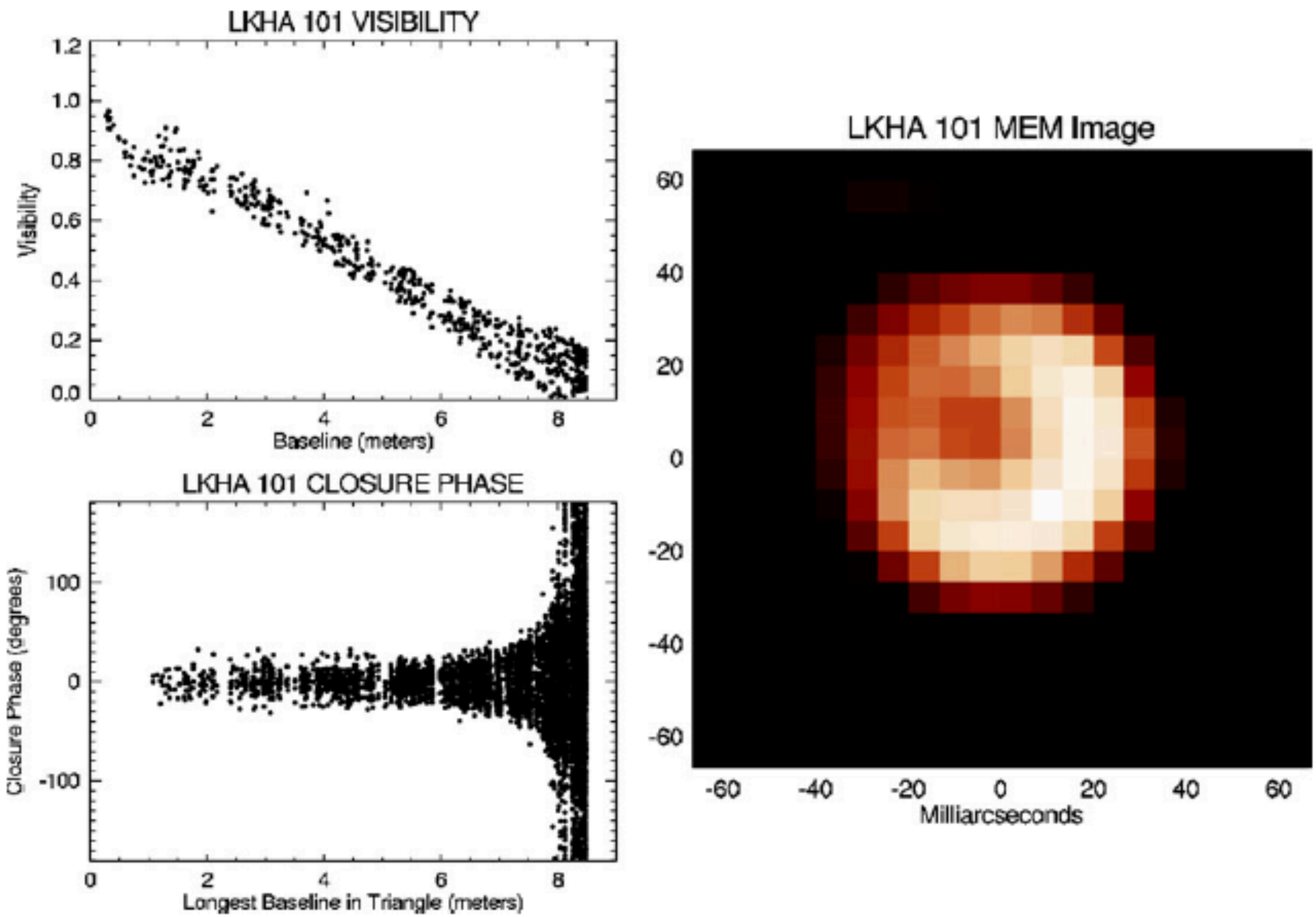

Interferometry on a single aperture

OUTLINE:

Why interferometry on a single aperture ?
- advantage of interferometric techniques on single aperture telescopes: high precision measurements enabled by good calibration

Aperture masking
(slides adapted from presentation by Frantz Martinache)

Pupil remapping

Interferometry as a technique to analyze single aperture short exposures:
- Speckle interferometry

Interferometry on a single aperture: First Aperture Masking experiment

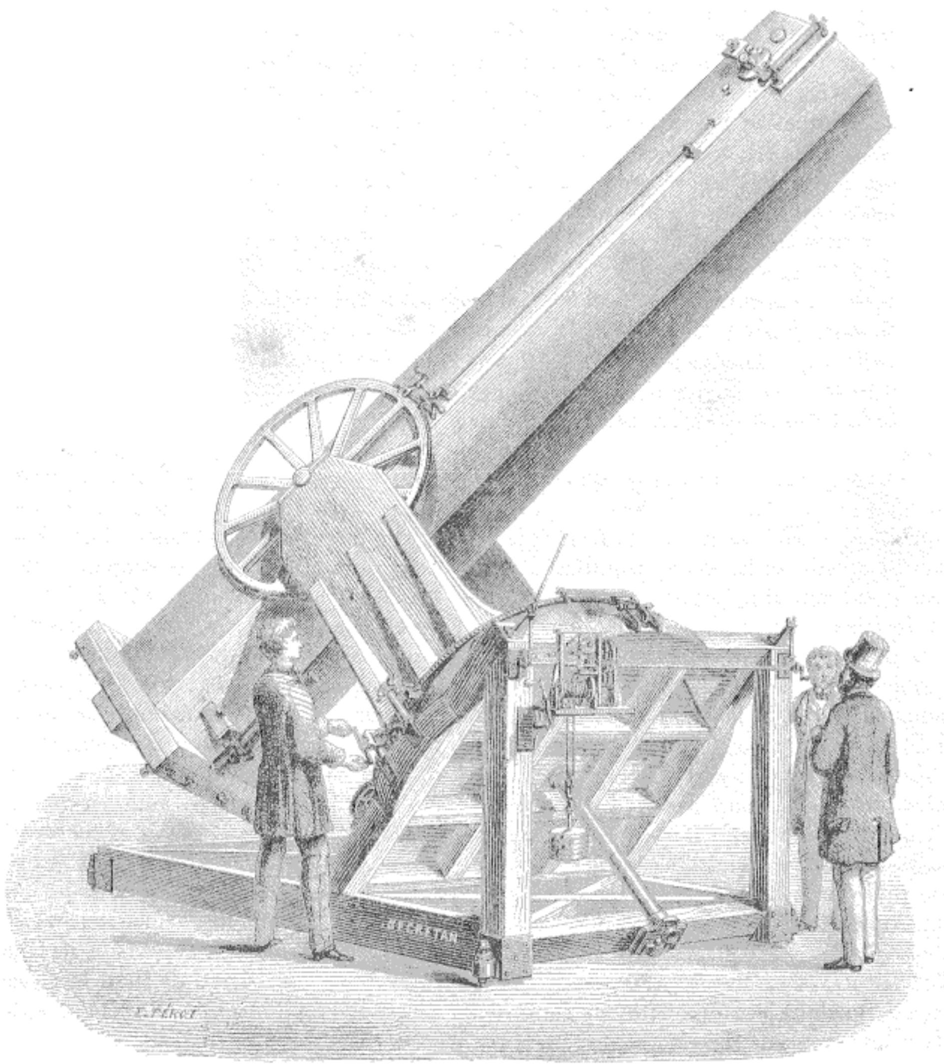

Le grand télescope Foucault, de l'Observatoire de Marseille.

<u>Marseille 1873</u>,
Edouard Stephan
attempts at measuring
the diameter of stars.

Baseline of 80 cm,
∅★ < 0.16”

Michelson later improved the experiment with an beam expanding the baseline, and was the first to resolve stars

Aperture masking: principle

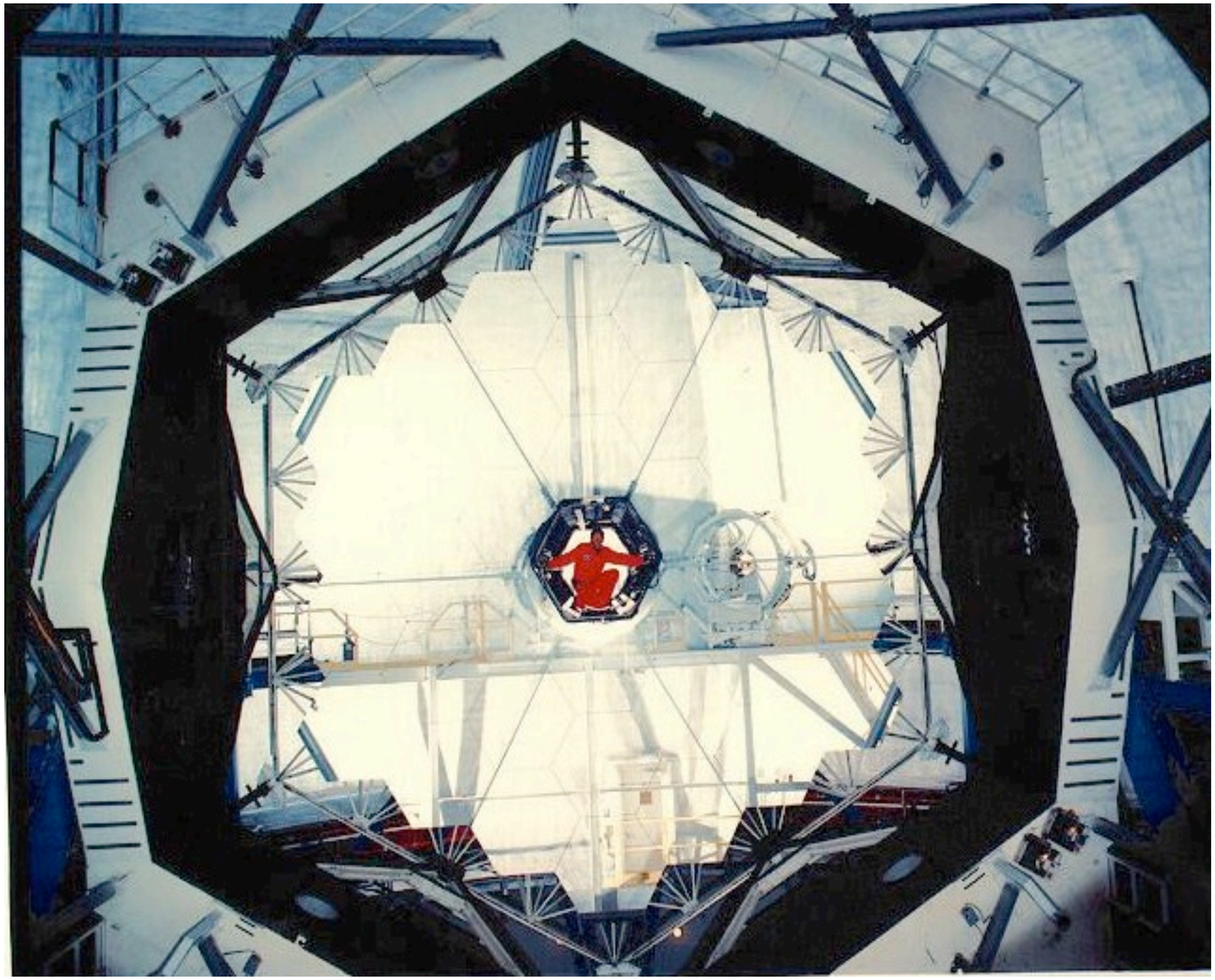

Aperture masking: principle

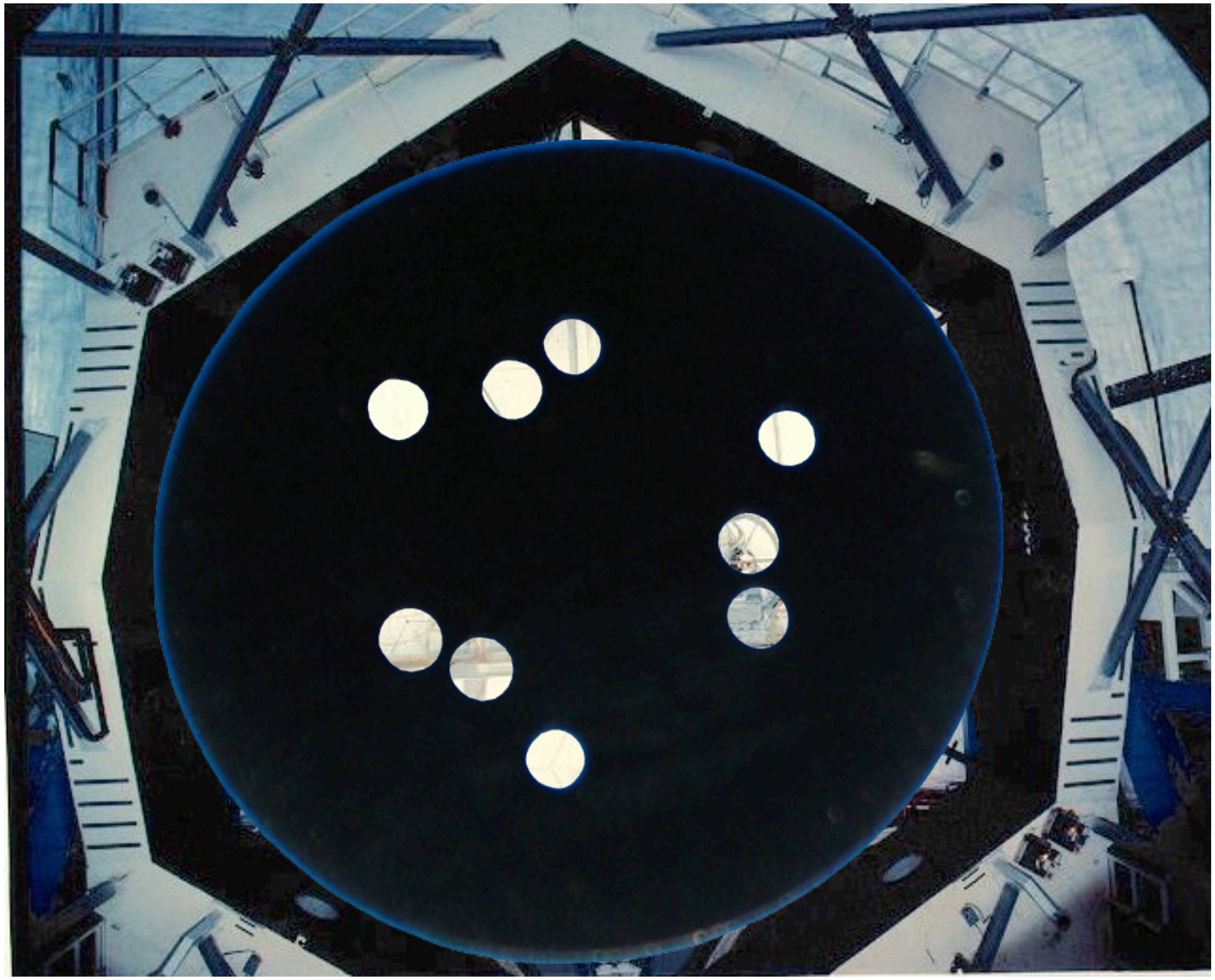

ref: Tuthill et al, 2000, PASP, 112, 555

Fizeau Interferometry

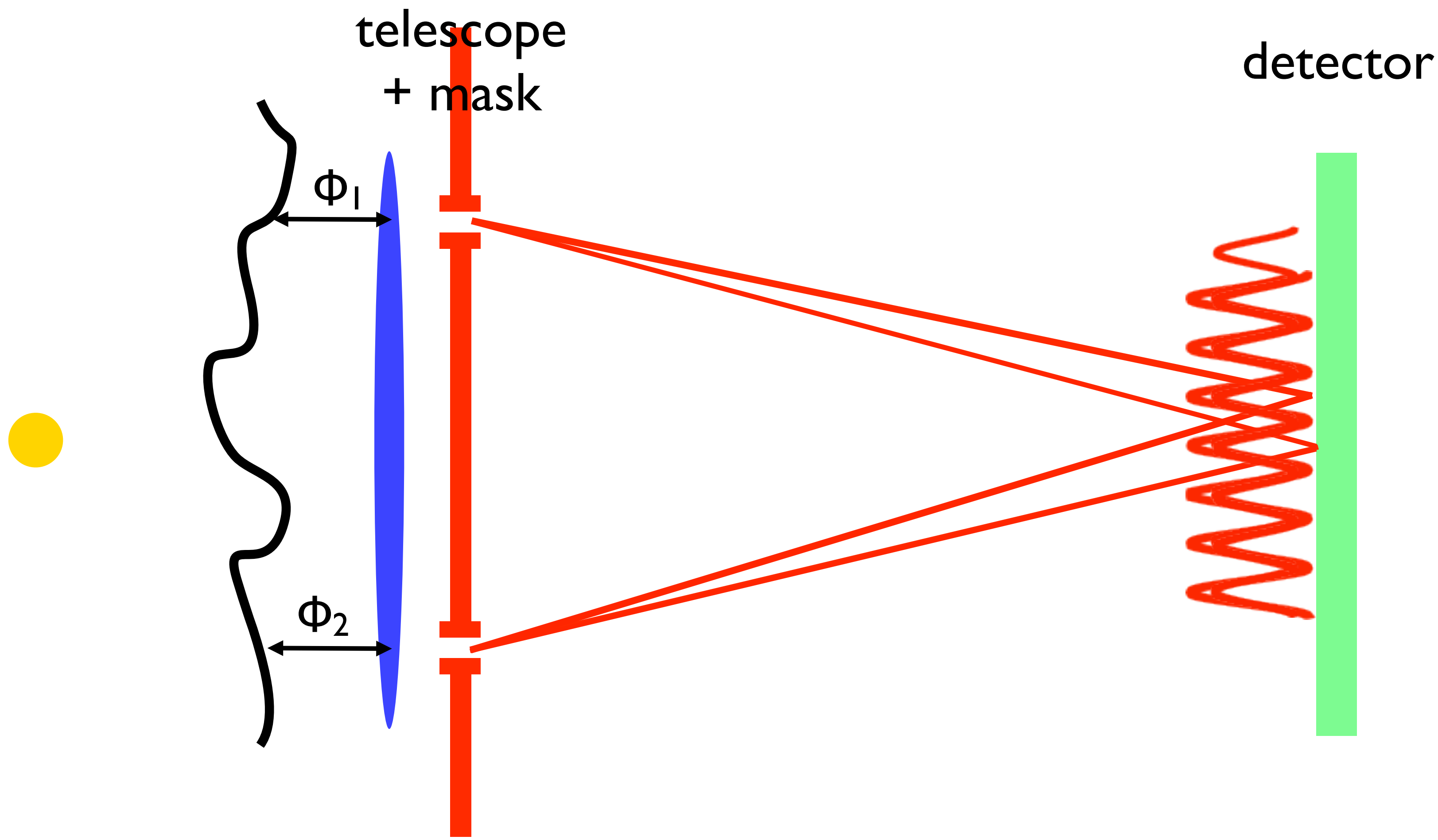

visibility:

$0 < V^2 < 1$

phase:

$\Phi = \Phi_0 + (\Phi_1 - \Phi_2)$

Redundancy: Atmosphere affects the phases, Redundancy destroys the amplitudes

Redundant

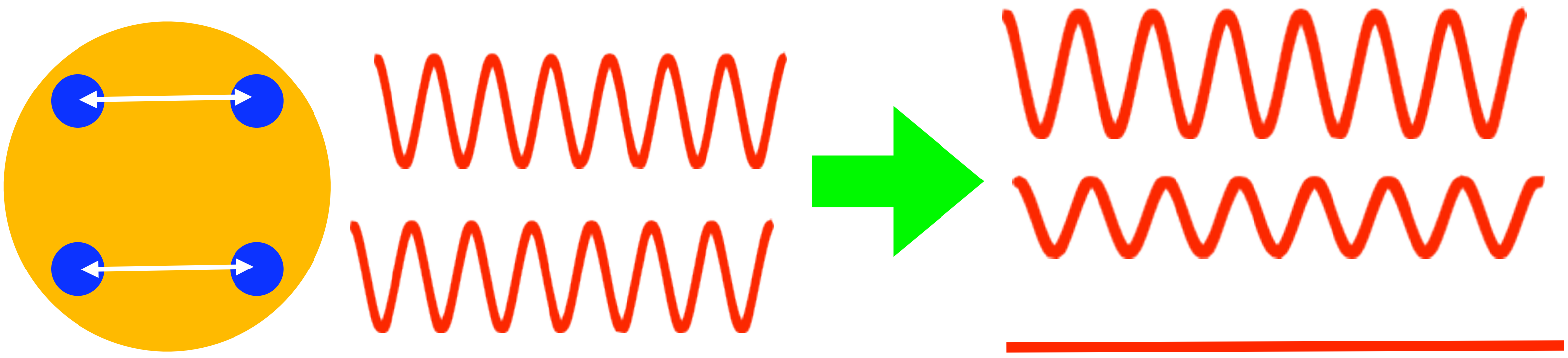

fringe amplitude is function of phase offset between baselines
→ **visibilities and phases cannot be measured**

Non Redundant

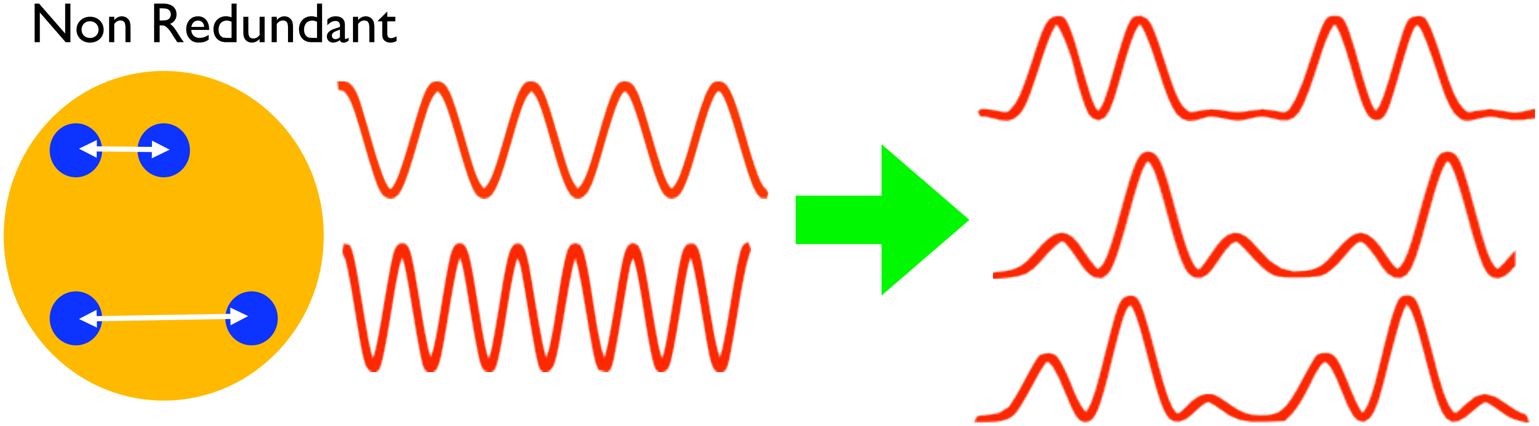

different baselines at different frequencies
→ **visibilities and phases can be isolated by Fourier Transform**

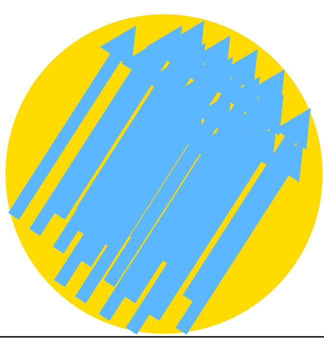

A full aperture is very redundant

Aperture Masking: creating non-redundant aperture with pupil mask

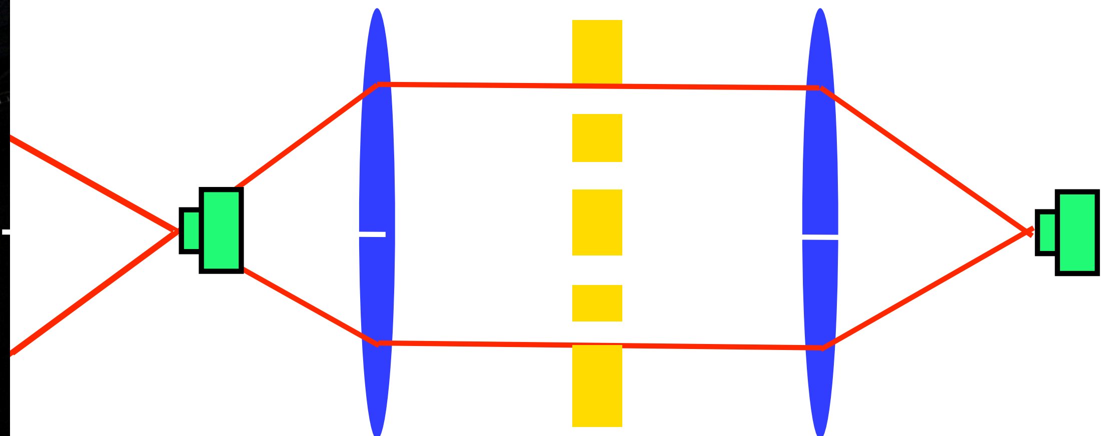

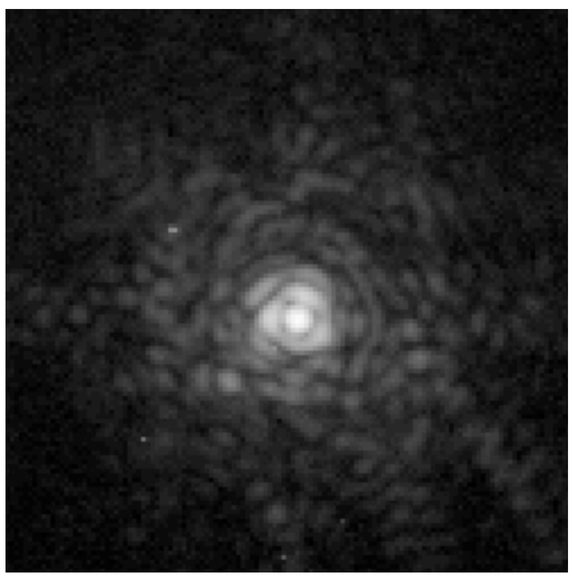

Image and Fourier planes

conventional imaging

aperture masking

Image

$|FT|^2$

Modulation Transfer Function

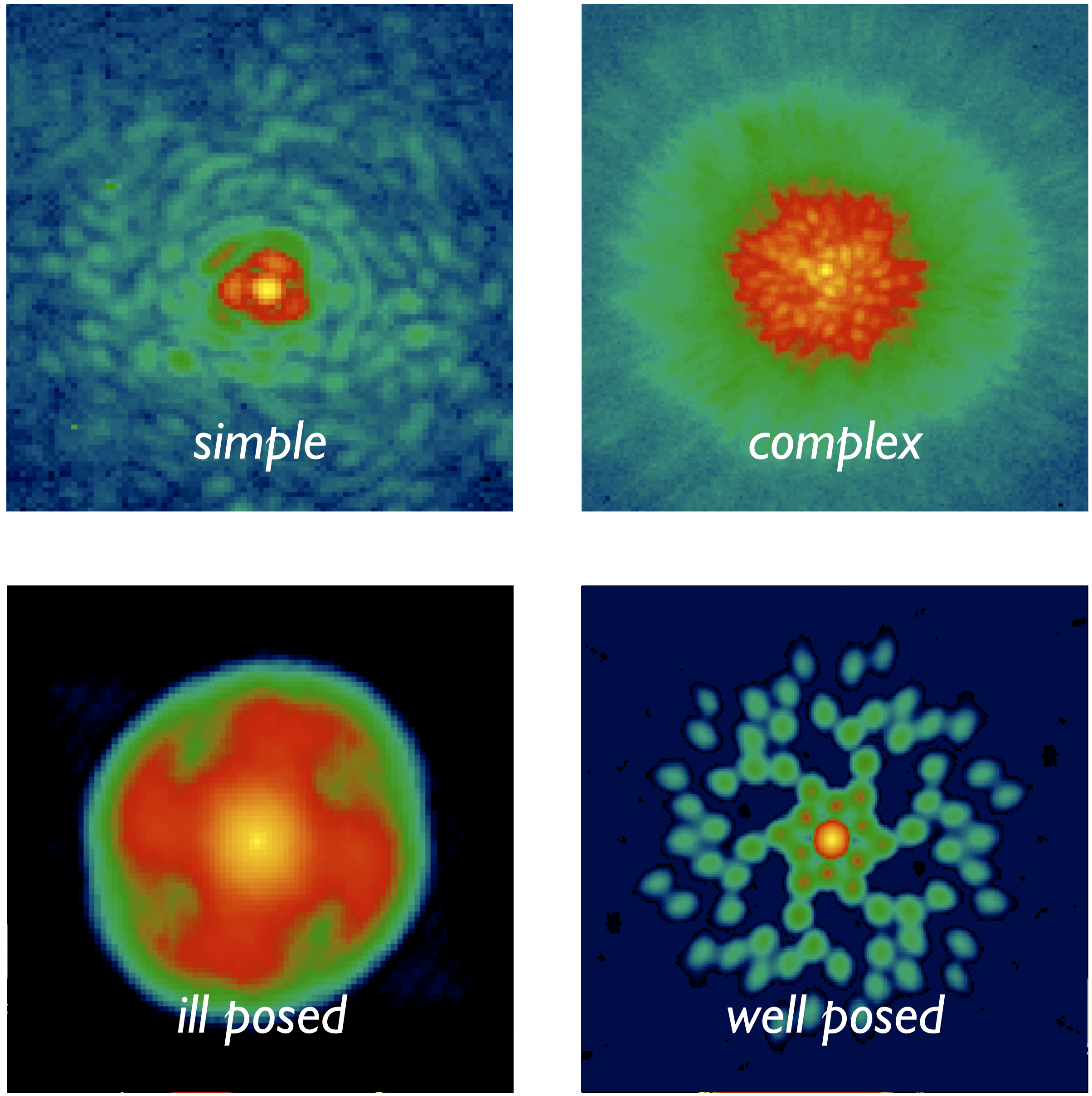

A neat trick: the closure phase

9-hole mask
36 visibilities
84 triangles
(28 independent)

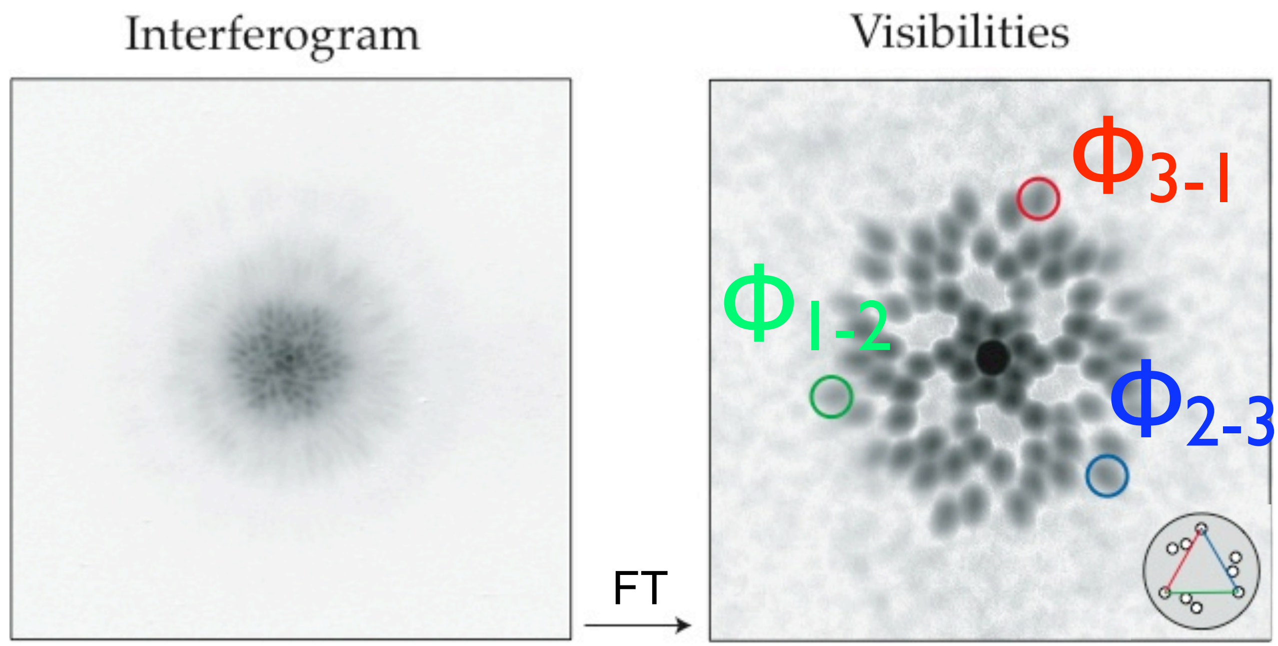

$\Phi(1\text{-}2) = \Phi(1\text{-}2)_0 + (\Phi_1 - \Phi_2)$

$\Phi(2\text{-}3) = \Phi(2\text{-}3)_0 + (\Phi_2 - \Phi_3)$

$\Phi(3\text{-}1) = \Phi(3\text{-}1)_0 + (\Phi_3 - \Phi_1)$

measured = intrinsic + atmospheric

Closure phases are invariant to atmospheric phase

cancels out in closure phase sum

Binary systems

3 parameters: angular separation, position angle, contrast
Error estimate: closure phase scattering
Small systematic error

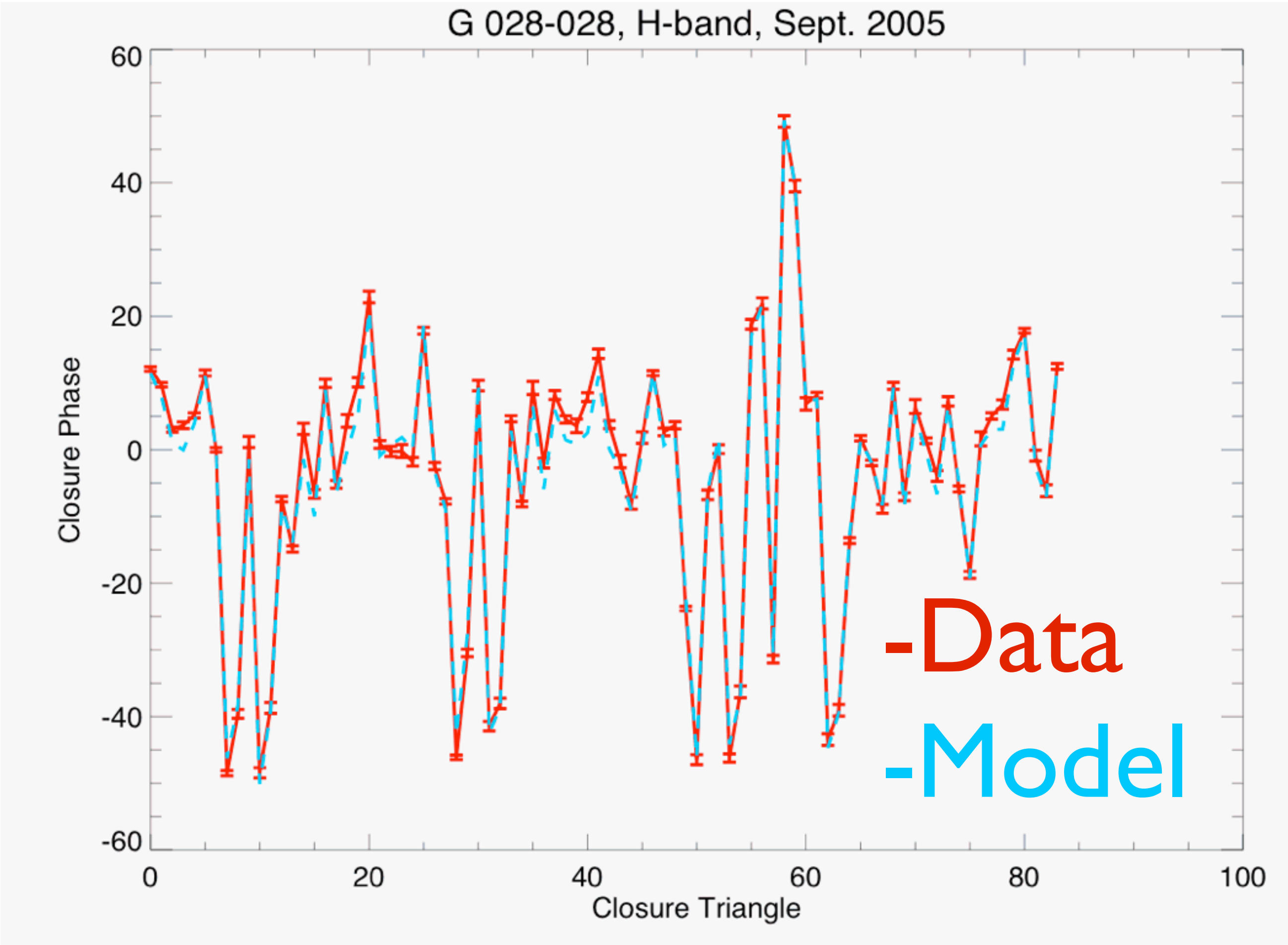

40 % strehl
0.3 deg scatter
stability ~ λ/1000
all passive !

An example of super-resolution

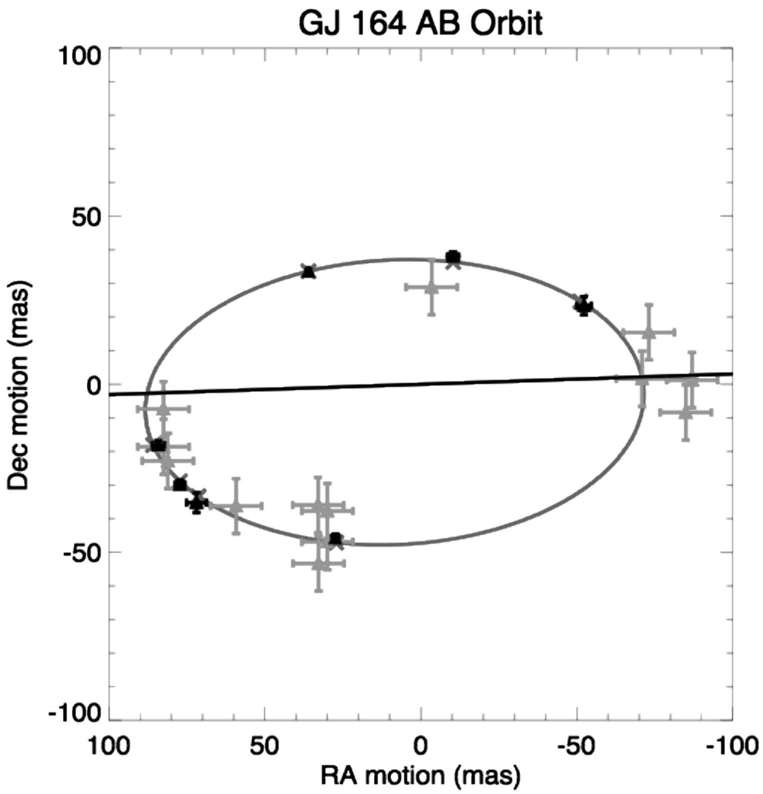

Black points: masking measurements
Grey points: STEPS astrometry

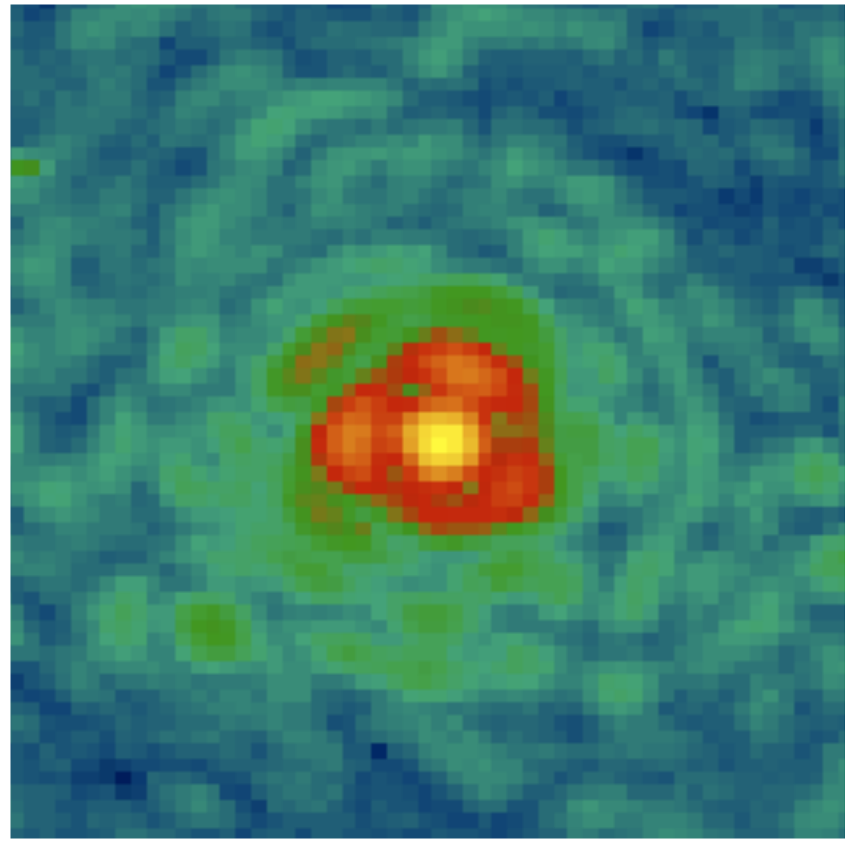

H-band image of GJ164 by the Hale Telescope

λ/D = 66 mas

Example result

LkCa 15: A Young Exoplanet Caught at Formation? (Kraus & Ireland 2012)

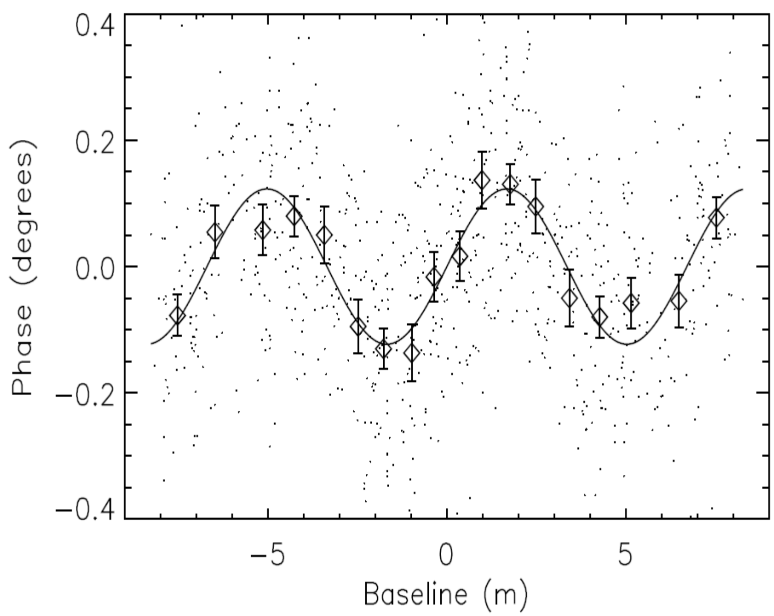

FIG. 1.— Fourier phase fitted to closure-phase (small dots) and the binned version of the same observable (triangles) for all 2010 K-band data on LkCa 15, plotted against the baseline projected along the principle axis of the best fit binary model. The phases of the best fit binary model model from Table 2 is shown as a solid line..

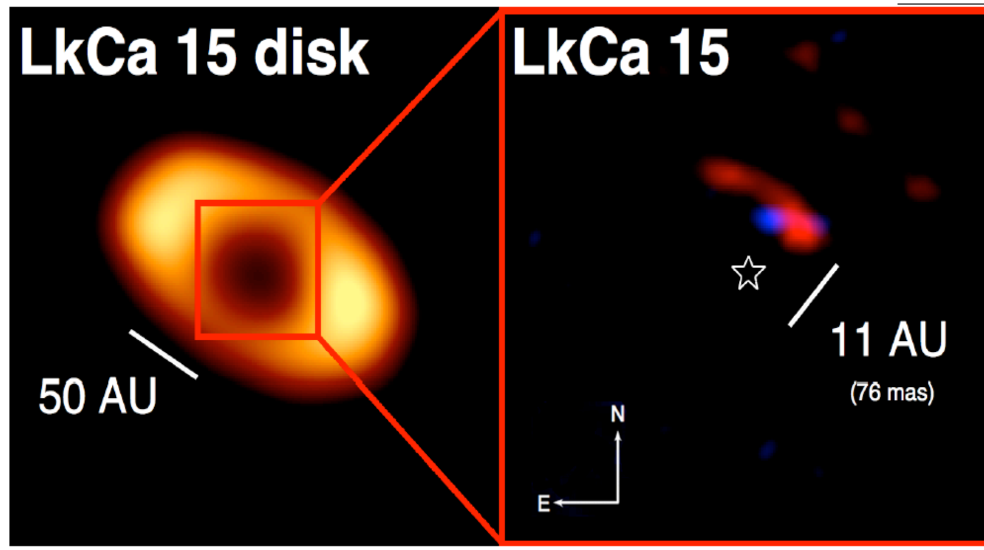

FIG. 3.— Left: The transitional disk around LkCa15, as seen at a wavelength of 850 μm (Andrews et al. 2011). All of the flux at t wavelength is emitted by cold dust in the disk; the deficit in the center denotes an inner gap with radius of ∼55 AU. Right: An expand view of the central part of the cleared region, showing a composite of two reconstructed images (blue: K' or $\lambda = 2.1$ μm, from Novem 2010; red: L' or $\lambda = 3.7$ μm, from all epochs) for LkCa 15. The location of the central star is also marked. Most of the L' flux appears come from two peaks that flank a central K' peak, so we model the system as a central star and three faint point sources.

Closure phases + fit for binary model

Reconstructed image (right)